Original Article

MOLECULAR METABOLISM

Adipocyte Xbp1s overexpression drives uridine production and reduces obesity

Yingfeng Deng [1], Zhao V. Wang [2], Ruth Gordillo [1], Yi Zhu [1], Aktar Ali [1], Chen Zhang [1], Xiaoding Wang [2,7], Mengle Shao [1], Zhuzhen Zhang [1], Puneeth Iyengar [3], Rana K. Gupta [1], Jay D. Horton [4], Joseph A. Hill [2,5], Philipp E. Scherer [1,6,*]

ABSTRACT

Objective: The spliced transcription factor Xbp1 (Xbp1s), a transducer of the unfolded protein response (UPR), regulates lipolysis. Lipolysis is stimulated by fasting when uridine synthesis is also activated in adipocytes.
Methods: Here we have examined the regulatory role Xbp1s in stimulation of uridine biosynthesis in adipocytes and triglyceride mobilization using inducible mouse models.
Results: Xbp1s is a key molecule involved in adipocyte uridine biosynthesis and release by activation of carbamoyl-phosphate synthetase 2, aspartate transcarbamylase, dihydroorotase (CAD), the rate-limiting enzyme for UMP biosynthesis. Adipocyte Xbp1s overexpression drives energy mobilization and protects mice from obesity through activation of the pyrimidine biosynthesis pathway.
Conclusion: These observations reveal that Xbp1s is a potent stimulator of uridine production in adipocytes, enhancing lipolysis and invoking a potential anti-obesity strategy through the induction of a futile biosynthetic cycle.

Keywords Obesity; Xbp1; ER stress; UPR; Pyrimidine; Uridine; CAD

1. INTRODUCTION

Pyrimidines are critical for cell proliferation and growth [1]. Cells can obtain pyrimidine through *de novo* synthesis or through a salvage pathway. Plasma uridine is found at concentrations much higher than other nucleosides and provides sufficient uridine for cells that depend on an exogenous supply of uridine to meet basic cellular anabolic needs [2]. Liver has been viewed the major organ for homeostatic regulation of plasma uridine [3]. We have recently demonstrated that liver and adipose tissue are both critical for the maintenance of plasma uridine levels [4]. Under fasting conditions, plasma uridine concentrations double. Even though only moderate in terms of the magnitude of the change, the doubling of uridine concentrations has major implications for temperature regulation and energy homeostasis [4]. This fasting-induced increase of plasma uridine relies on pyrimidine biosynthesis in adipocytes, which occurs concomitantly with high levels of lipolysis. However, we do not know whether these two processes are mechanistically linked in adipocytes.

Lipolysis is a highly regulated process in adipocytes aimed at triglyceride mobilization and fatty acid release, thereby playing a critical role in the survival of mammals during limited food supply [5]. Lipolysis is de-repressed by low levels of insulin and multiple enzymes locally within adipocytes that need to be activated to effectively engage in the lipolytic process [6]. ER stress, a condition when unfolded protein builds up in the endoplasmic reticulum (ER), has been widely associated with the development of insulin resistance at the cellular level [7]. Drugs that trigger ER stress can increase lipolysis in adipocytes [8]. However, we do not understand how ER stress regulates lipolysis *in vivo*. Intriguingly, Xbp1s, a transcriptional factor that is activated in response to ER stress [9], is elevated in subcutaneous fat tissue from obese human subjects [7], suggesting Xbp1s induction as a possible link between ER stress and obesity. However a recent report indicated that the loss of Xbp1 in adipocytes does not affect overall adiposity in mice, but mobilization of TGs from adipocytes during lactation for milk production was significantly impaired in these animals, reflecting a possible specific role of Xbp1s in stimulating lipolysis during lactation [10].

We found that although the expression of Xbp1s in adipocytes is induced by a number of lipolytic stimuli, lipolysis *per se* is not dependent on Xbp1s. Conversely, adipocyte overexpression of Xbp1s leads to profound loss of fat mass, and this loss is associated with elevation of uridine in adipose tissue and blood circulation. We found Xbp1s is a potent activator of *Cad*, the rate-limiting enzyme for uridine biosynthesis. Inhibition of full-length CAD expression in the adipocyte mitigates the weight loss effect induced by Xbp1s. This demonstrates

[1]Touchstone Diabetes Center, Department of Internal Medicines, University of Texas Southwestern Medical Center, Dallas, TX, 75390, USA [2]Division of Cardiology, Department of Internal Medicine, University of Texas Southwestern Medical Center, Dallas, TX, 75390, USA [3]Department of Radiation Oncology, University of Texas Southwestern Medical Center, Dallas, TX, 75390, USA [4]Department of Molecular Genetics, University of Texas Southwestern Medical Center, Dallas, TX, 75390, USA [5]Department of Molecular Biology, University of Texas Southwestern Medical Center, Dallas, TX, 75390, USA [6]Department of Cell Biology, University of Texas Southwestern Medical Center, Dallas, TX, 75390, USA [7]Department of Cardiology, Renmin Hospital of Wuhan University, Wuhan, China

*Corresponding author. Touchstone Diabetes Center, Departments of Internal Medicine and Cell Biology, UT Southwestern Medical Center, Dallas, TX, 75390, USA. Fax: +214 648 8720. E-mail: Philipp.Scherer@utsouthwestern.edu (P.E. Scherer).

Received February 12, 2018 • Revision received February 26, 2018 • Accepted February 26, 2018 • Available online 2 March 2018

https://doi.org/10.1016/j.molmet.2018.02.013

that Xbp1s triggered fat mass loss relies on pyrimidine biosynthesis. Since uridine biosynthesis needs to be orchestrated at multiple levels, from substrate availability to mitochondrial biosynthetic function, a dysregulation of uridine biosynthesis at the level of the adipocyte might lead to obesity even in the presence of Xbp1s induction. Based on the chronic weight loss effects we observe due to adipocyte Xbp1s overexpression, we propose that the stimulation of the adipocyte uridine synthesis pathway is a potential therapeutic target area for the treatment of obesity.

2. MATERIALS AND METHODS

2.1. Animals and experimental protocol

Animals were maintained on a 12 h dark/light cycle from 6 AM to 6 PM. C57BL/6 inbred mice and leptin deficient mice (*ob/ob*) were housed in individually ventilated cages with free access to water and food. Mice were maintained on standard rodent chow diet (2916, Teklad) and were switched to special diet at 8 weeks old if not specified. High fat diet (D12492, Research Diet) was used for diet-induced obesity in mice. Doxycycline-containing chow diet or high fat diet (600 mg/kg, Bio-serv) was used to induce gain- or loss-of function of genes via tet-on system. All the experiments were performed after mice were switched to Dox feed for 2–4 weeks unless specified. The Institutional Animal Care and the Use Committee of University of Texas Southwestern Medical Center has approved all animal experiments.

The TRE-Xbp1s mouse model in FVB background had been bred to C57/B6 background for more than 9 generations [11] before crossing with the adiponectin promoter driven rtTA transgenic mouse [12] to generate the adipocyte-specific **f**at **i**nducible **X**bp1**s** overexpression (FIXs) mouse model. The mice harboring TRE-Cre [13] and Adiponectin promoter driven rtTA transgenes were crossed to $Xbp1^{fl/fl}$ mice [14] to generate adipocyte-specific **f**at **i**nducible **X**bp1 **k**nock**o**ut (FIX KO) mouse model. The mice harboring TRE-Cre, TRE-Xbp1s and Adiponectin promoter driven rtTA transgenes were crossed to $Cad^{fl/fl}$ mice [4] to generate FIXs, Cad KO mice. The sex and age-matched littermates of the FIXs, FIX KO, or FIXs, Cad KO mice were used as controls respectively. The $Cad^{fl/fl}$ mice were derived from ES clone (EPD0282_2_F10) from UCDAVIS KOMP Repository at the transgenic core in UTSW.

CL 316,243 (Sigma) was prepared in 1 × PBS and administered intraperitoneally at 1 mg/kg bodyweight to mice. Plasma and tissues were harvested 2 h post injection. To induce cachexia, C57BL/6 mice at 2–3 months of age were injected with 1×10^7 syngeneic Lewis Lung Carcinoma (LLC) cells in 1 × PBS into animal flanks. The control mice received 1 × PBS injection only. The mice were then evaluated for tumor growth with caliper measurements and small animal CT, weight loss, and fat and muscle volumes measured by small animal ECHO MRI weekly. When there was up to 10–20% weight loss with concomitant 40–50% adipose loss, frank cachexia was established with induced adipocyte lipolysis development. To avoid severe sickness and to study the early event in lipolysis development, animals were sacrificed 3 weeks post injection when the fat mass loss was within a range of 10%.

2.2. MRI, metabolic cage studies, CT scan, and body temperature measurement

Accurate determination of body composition was conducted using nuclear magnetic resonance (Bruckner Minispec mq10). Metabolic cage studies were performed in the UTSW Mouse Metabolic Phenotyping Core using the CLAMS system (Columbus Instrument) as described previously [11]. Prior to measurements, mice were allowed to acclimatize to the metabolic cages for five days. CT-Scanning was performed with a MicroCT Scanner (GE Healthcare) in the UTSW Mouse Metabolic Phenotyping Core. Body temperature was measured using an IPTT-300 transponder implanted longitudinally above the shoulder of mouse (Bio Medic Data Systems).

2.3. ^{3}H-triolein uptake and β-oxidation *in vivo*

Tissue-specific lipid-uptake, and β-oxidation analysis were performed as previously described [15]. Briefly, ^{3}H-triolein was injected via tail vein (2 μCi/mouse in 100 μl of 5% intralipid). After 15 min, tissues were harvested, and lipids were extracted using a chloroform-to-methanol based extraction method. Samples were then counted for radioactivity in lipid and aqueous fractions.

2.4. Histology and metabolite measurements

Tissues were dissected and fixed in 4% paraformaldehyde overnight. Paraffin processing, embedding, sectioning, and standard hematoxylin and eosin (H&E) staining were performed by the histology core at UTSW. Images were acquired using Coolscope (Nikon). Plasma glucose levels were determined by an oxidase-peroxidase assay (Sigma). Serum free fatty acid and ketone bodies levels were determined by NEFA-HR and Autokit Total Ketone Bodies (Wako Pure Chemical Industries). Plasma and tissue uridine concentrations were examined by HPLC-MS/MS at UTSW Mouse Metabolic Phenotyping Core as described [4].

2.5. Isolation and differentiation of adipose stromal vascular culture and treatments

Stromal vascular cells isolation and adipocyte differentiation are performed as described [16]. Briefly, dissected subcutaneous adipose tissues from mice were washed, minced, and then digested for 2 h at 37 °C. SVF cells isolated were then plated onto collagen-coated dishes and cultured in 10% CO_2 at 37 °C in growth media containing DMEM/F12 (Invitrogen) and 10% FBS. For adipocyte differentiation, confluent cultures were exposed to the adipogenic cocktail supplemented with dexamethasone (1 μM), insulin (5 μg/mL), isobutylmethylxanthine (0.5 mM) and rosiglitazone (1 μM) in growth media for 48 h. After 48 h, cells were maintained in growth media containing insulin (5 μg/mL) and rosiglitazone (1 μM) until harvest. Post differentiation, doxycycline (0.5 μg/mL) was supplemented to growth media on day 6 to induce transgene expression. Tunicamycin (0.5 μg/mL) or Thapsigargin (0.5 μM) was supplemented to growth media on day 7 to induce ER stress. PALA was prepared in 0.9% NaCl and supplemented to cells on day 7 to inhibit *de novo* pyrimidine synthesis at different dose according to the description. PALA was synthesized as described previously [17] and verified for its efficacy *in vivo* [4].

2.6. RNA isolation and gene expression analysis

Mice were euthanized under fed condition unless specified. Tissues were harvested, frozen immediately in liquid nitrogen, and stored at −80 °C until use. Frozen tissues of 50–100 mg were homogenized, and total RNA was isolated using NucleoSpin RNA II mini columns (Macherey–Nagel). Total RNA (100 ng–1 μg) was used for reverse transcription with iScript (Bio-Rad). Relative gene expression was determined by quantitative PCR using SYBR Green PCR system (Roche), and values were normalized to 18s rRNA using the ΔΔ–Ct method. Primer sequences are provided in Supplementary Table 1 (Table S1).

2.7. Immunoblotting analysis

Frozen fat and liver samples were homogenized in T-PER buffer (Thermo Scientific) and supplemented with complete protease inhibitor

cocktail (Roche) and phosphoSTOP (Roche). After clearing the samples at 14,000 RPM for 10 min at 4 °C, protein concentrations were measured by BCA Assay (Thermo Scientific). Nuclear extract was prepared using NE-PER kit (Thermo Scientific). Adipocyte isolation from sWAT was performed similar to stromal vascular cells isolation except for the cell collection is conducted for floating adipocytes. Equal amounts of total protein from each sample were mixed with Laemmli sample buffer, resolved on 4–20% Tris-glycine gels (Bio-Rad), followed by transfer to nitrocellulose membranes. Membranes were then incubated with primary antibodies overnight at 4 °C. The following antibodies were used: GAPDH and Xbp1 from Santa Cruz; Lamin A/C, and CAD from Cell Signaling. IRDye 800-conjugated anti-rabbit (Li-Cor), IRDye 700-conjugated anti-goat (Rockland) or Alexa Fluor 680-conjugated anti-mouse secondary antibodies (Invitrogen) were used. Membranes were scanned and processed using a LI-COR Odyssey infrared imaging system (Li-Cor).

2.8. Statistical analysis

Results are reported as mean ± SEM. Statistical analysis of the data was performed with two-tailed *t* test. Paired *t* test was performed for samples collected from the same mouse during a time course study. A p value < 0.05 was considered as significant. All analyses were performed using GraphPad Prism Software 7.01 (GraphPad Software, Inc.)

3. RESULTS

3.1. Adipose tissue Xbp1s induction associates with lipolysis

Xbp1s, an ER stress transducer, is critical for lipolysis during lactation [10]. To understand the physiological relevance of Xbp1s for lipolysis and pyrimidine synthesis, both activities that are relevant in the fasting adipocyte [4], we measured gene expression of Xbp1s in adipose tissue under these conditions. We observed that fasting caused a 2-to-4-fold increase of Xbp1s in epididymal white adipose tissue (eWAT), subcutaneous white adipose tissue (sWAT), and interscapular brown adipose tissue (BAT) in wild type C57Bl/6 mice (Figure 1A). This is in sharp contrast to the liver, where Xbp1s is induced by refeeding and suppressed by fasting [11]. We also analyzed Xbp1s gene expression in fat depots from mice undergoing acute lipolysis by treatment with CL316,243, a β3 adrenergic receptor agonist. We found that the treatment with the CL compound increased the expression of Xbp1s 10-fold in both WATs and BAT within 2 h post administration (Figure 1B). In contrast to acute lipolytic states, cachexia is a condition associated with chronically increased lipolysis. To test whether Xbp1s

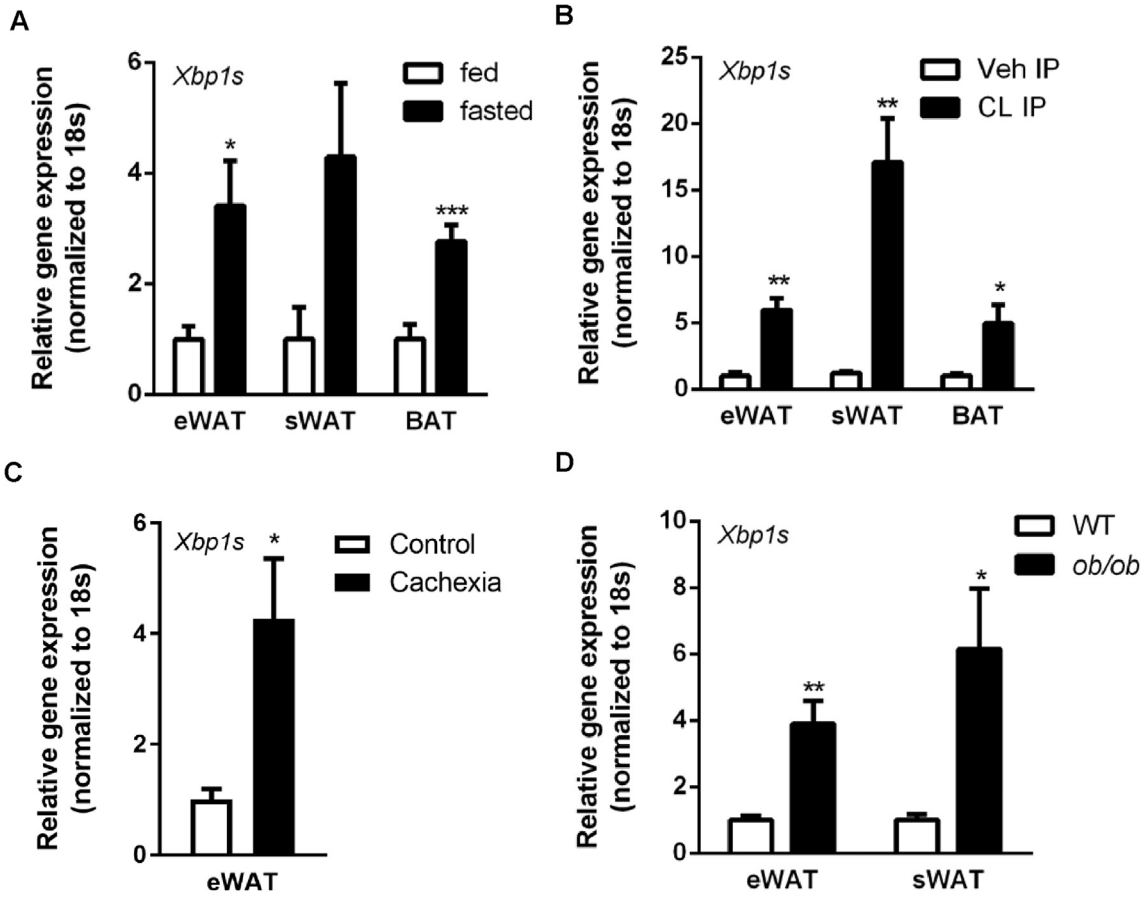

Figure 1: Xbp1s induction in adipocyte associates with lipolysis. (A) Xbp1s mRNA levels in fat pads were elevated after an overnight fast compared to fed group (n = 4). (B) Xbp1s mRNA levels in fat pads were elevated upon β3 adrenergic receptor stimulation with CL 316,243 compared to vehicle injected group (n = 4). (C) Xbp1s mRNA levels in fat pads were elevated in mice undergoing LLC tumor-induced cachexia compared to control group (n = 5). (D) Xbp1s mRNA levels in fat pads were elevated in *ob/ob* mice compared to lean littermates (n = 5). eWAT, epididymal white adipose tissue. sWAT, subcutaneous white adipose tissue. BAT, interscapular brown adipose tissue. Data were analyzed with two-tailed Student *t* test. *, $p < 0.05$; **, $p < 0.01$, ***, $p < 0.001$. Error bars denote SEM.

is elevated in adipose tissue when lipolysis is stimulated with a chronic challenge, we analyzed Xbp1s gene expression in a mouse model with cachexia (induced through subcutaneous implantation of tumorigenic cells). We found that the expression of Xbp1s was elevated 4-fold in eWAT from mice with cachexia (Figure 1C). Lastly, leptin is a critical adipokine involved in plasma uridine homeostasis [4]. Since leptin deficiency is also associated with elevated lipolysis, we analyzed Xbp1s expression in the leptin-deficient *ob/ob* mice. We found Xbp1s levels were increased 4-to-5-fold in eWAT and sWAT samples isolated from *ob/ob* mice (Figure 1D). Together, our data indicate that Xbp1s induction in adipose tissue is closely tied to lipolysis. This correlation opens up the possibility that adipocyte Xbp1s might be induced when uridine biosynthesis is activated by fasting [4].

3.2. Adipocyte Xbp1s regulates plasma uridine elevation

Adipose tissue contains multiple cell types in addition to adipocytes. To study the role of adipocyte Xbp1s in lipolysis and uridine biosynthesis, we generated a mouse model with adipocyte-specific **f**at tissue **i**nducible **X**bp1**s** overexpression (referred as FIXs mice) (Figure 2A). The FIXs mouse harbors a transgene for adipocyte-specific rtTA

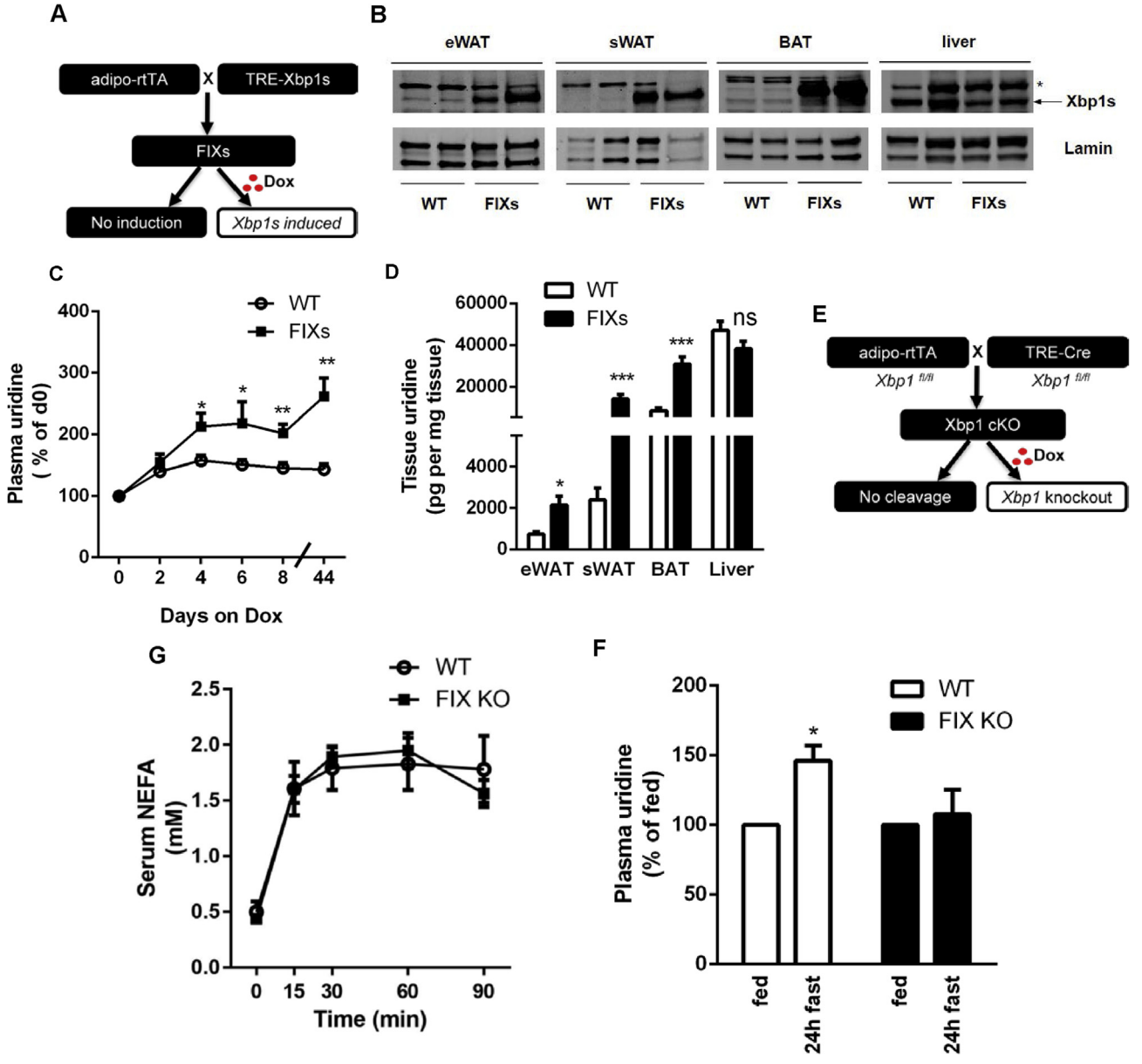

Figure 2: Adipocyte Xbp1s is sufficient and necessary for plasma uridine elevation triggered by lipolysis. (A) Strategy for the generation of mouse with adipocyte-specific **f**at tissue **i**nducible **X**bp1**s** overexpression (FIXs). (B) Verification of Xbp1s expression by western blotting after 7 days of Dox chow feeding. Lamin was used as a loading control. * denotes a non-specific cross-reacting band. (C) Adipocyte Xbp1s overexpression increased plasma uridine levels (n = 5–6). Plasma uridine concentration from each mouse was normalized to basal level prior to Dox. Statistical analysis was performed for the two genotypes at time points indicated. (D) Adipocyte Xbp1s overexpression increased uridine concentration in fat depots (n = 6). (E) Strategy for the generation of mouse with adipocyte-specific **f**at tissue **i**nducible **X**bp1 **k**nock**o**ut (FIX KO). (F) Adipocyte Xbp1 deficiency prevented plasma uridine elevation in fasted mice (n = 3). Statistical analysis was performed for each genotype using the fed state of that group as base line. (G) Serum NEFA was increased by CL316, 243 in both WT and FIX KO mice (n = 3). Data in (C), (D), and (G) were analyzed with two-tailed Student *t* test, and data in (F) was analyzed with paired *t* test. *, $p < 0.05$; **, $p < 0.01$, ***, $p < 0.001$. Error bars denote SEM.

expression driven by the adiponectin promoter and a transgene for Xbp1s driven by a tet-on cassette. Induction of Xbp1s adipocyte-specifically is achieved through doxycycline (Dox) containing feed. 48 h post switch to Dox-containing food, a robust induction of Xbp1s protein was detected in both WATs and BAT from the FIXs mice, but not in liver (Figure 2B). Upon induction, the FIXs mice acutely increased plasma uridine levels twofold, and the mice maintained elevated levels of plasma uridine as long as they were kept on Dox chow (Figure 2C). FIXs mice displayed higher uridine concentrations than WT mice in eWAT, sWATs, and in BAT (Figure 2D), consistent with an increase in uridine biosynthesis in adipocytes. Liver, lacking ectopic Xbp1s expression, did not show a difference in uridine content, confirming that the change in tissue uridine content is selective for adipose tissue (Figure 2D). The data above indicate that adipocyte Xbp1s is sufficient to drive pyrimidine synthesis and, as a result, causes an elevation in plasma uridine. To examine the necessity of adipocyte Xbp1 for maintaining the plasma uridine supply, we generated an adipocyte-specific **f**at tissue **i**nducible **X**bp1 **k**nock**o**ut mouse (referred as FIX KO) (Figure 2E). The knockout of Xbp1 in adipocytes is induced by Dox feeding using a strategy similar to the one used in the FIXs mice. We found the 24 h fasting-induced increase in plasma uridine was reduced in the FIX KO mice (Figure 2F). However, the FIX KO mice did not show a reduced lipolysis response to CL316,243 (Figure 2G), indicating that adipocyte Xbp1s, while relevant for uridine biosynthesis, is not necessary for β3 adrenergic stimulation of lipolysis.

3.3. Xbp1s and ER stress stimulate uridine synthesis through CAD

The elevated adipose tissue uridine content in FIXs mice suggests pyrimidine synthesis activity is elevated by Xbp1s. *De novo* pyrimidine synthesis requires three peptides: carbamoyl-phosphate synthetase 2, aspartate transcarbamylase and dihydroorotase (CAD), dihydroorotate dehydrogenase (DHODH), and UMP synthase (UMPS) [18]. To dissect how Xbp1s might affect pyrimidine synthesis at the level of transcription, we examined the gene expression profile of the three enzymes in adipose tissue and liver. *Cad*, the first and rate limiting enzyme, showed a 2-to-8-fold increase in fat depots from FIXs mice (Figure 3A), whereas *Dhodh* and *Umps* were unaltered (Figure 3B–C), indicating that *Cad* may be a potential target gene activated by Xbp1s. Consistent with the changes at the mRNA level, the *Cad* protein amounts were increased in FIXs mice, with sWAT showing a more substantial increase than eWAT (Figure 3D, see Supplemental Fig. 1 for original gels). To determine if Xbp1s can stimulate pyrimidine synthesis in adipocytes autonomously, we differentiated cells from the stromal vascular fraction (SVF) of adipose tissue, and induced gain- and loss-of function of Xbp1s *in vitro* through the supplementation of Dox post adipocyte differentiation. During the experiments, no difference in adipocyte differentiation and lipid accumulation was detected before and post Dox supplementation. 24 h post Dox supplementation, Xbp1s expression in FIXs adipocytes was elevated, associated with a 1.5-fold increase in *Cad* gene expression (Figure 3E). To examine the effects on uridine production, we sampled the growth media

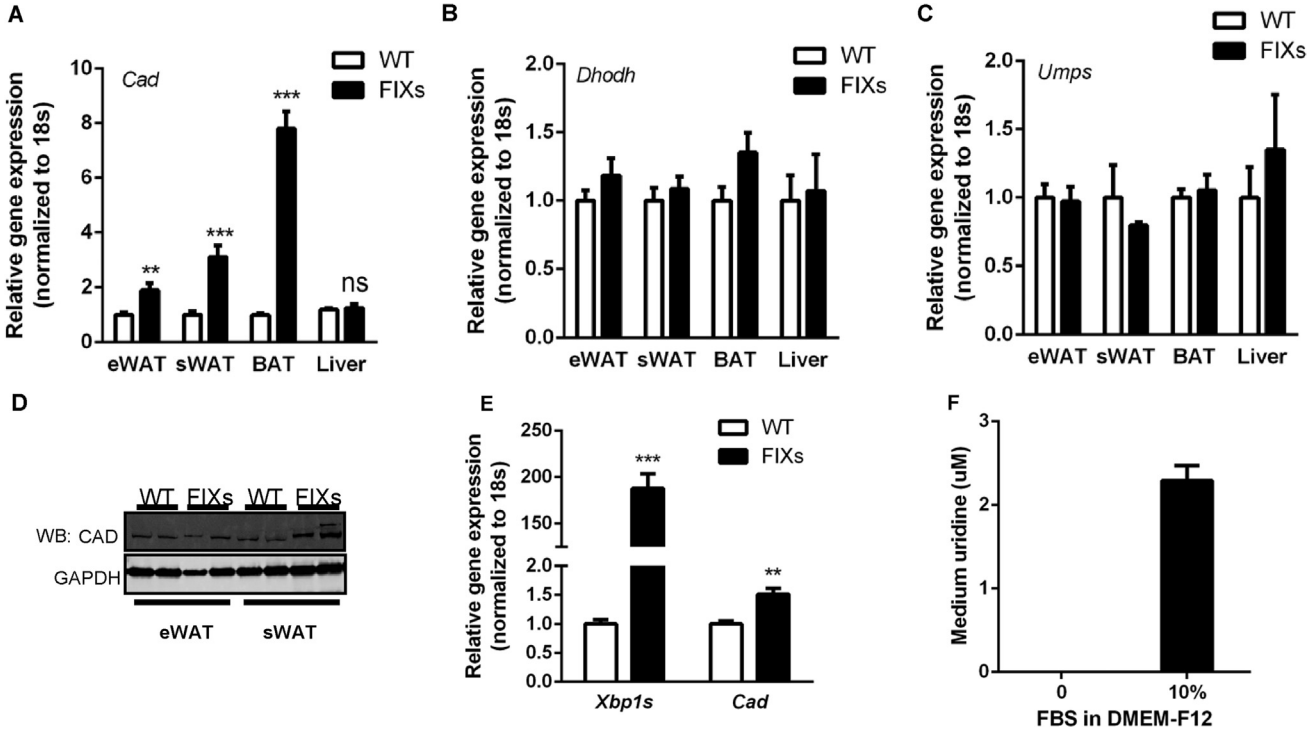

Figure 3: Xbp1s and ER stress regulates pyrimidine synthesis in adipocyte. (A) Adipocyte Xbp1s overexpression increased *Cad* mRNA in fat depots (n = 8). (B) Adipocyte Xbp1s overexpression did not change *Dhodh* mRNA in fat depots (n = 8). (C) Adipocyte Xbp1s overexpression did not change *Umps* mRNA in fat depots (n = 8). (D) Adipocyte Xbp1s overexpression induced elevation of Cad protein as assessed by immunoblotting. GAPDH was used as loading control. (E) *Cad* expression was increased by Xbp1s overexpression *in vitro* (24 h incubation with Dox). Adipocytes were differentiated from SVF and Dox were supplemented at day 6 post differentiation (n = 6). (F) Fetal Bovine Serum (FBS) but not DMEM contained uridine (n = 3) (G) Concentrations of uridine in cell culture medium were elevated by Xbp1s overexpression at 48 h post Dox addition (n = 3) and serum starvation (n = 3) (H) Concentrations of uridine in tissue culture medium were elevated by ER stress inducer treatment (n = 3). (I) Tunicamycin (TM) induced elevation of uridine in culture medium were suppressed by PALA in WT adipocyte but not Xbp1-knockout adipocytes (FIX KO). PALA was added at 0.1 μM, 10 μM, and 1 mM. (n = 3). (J) Xbp1s overexpression increased *Cad* mRNA in liver and heart (n = 3–6). LIXs, hepatocyte-specific **l**iver **i**nducible **X**bp1**s** overexpression mouse as described [11]. HIXs, cardiomyocyte-specific **h**eart **i**nducible **X**bp1**s** overexpression mouse as described [20]. Data were analyzed with two-tailed Student *t* test. *, $p < 0.05$; **, $p < 0.01$, ***, $p < 0.001$. Error bars denote SEM.

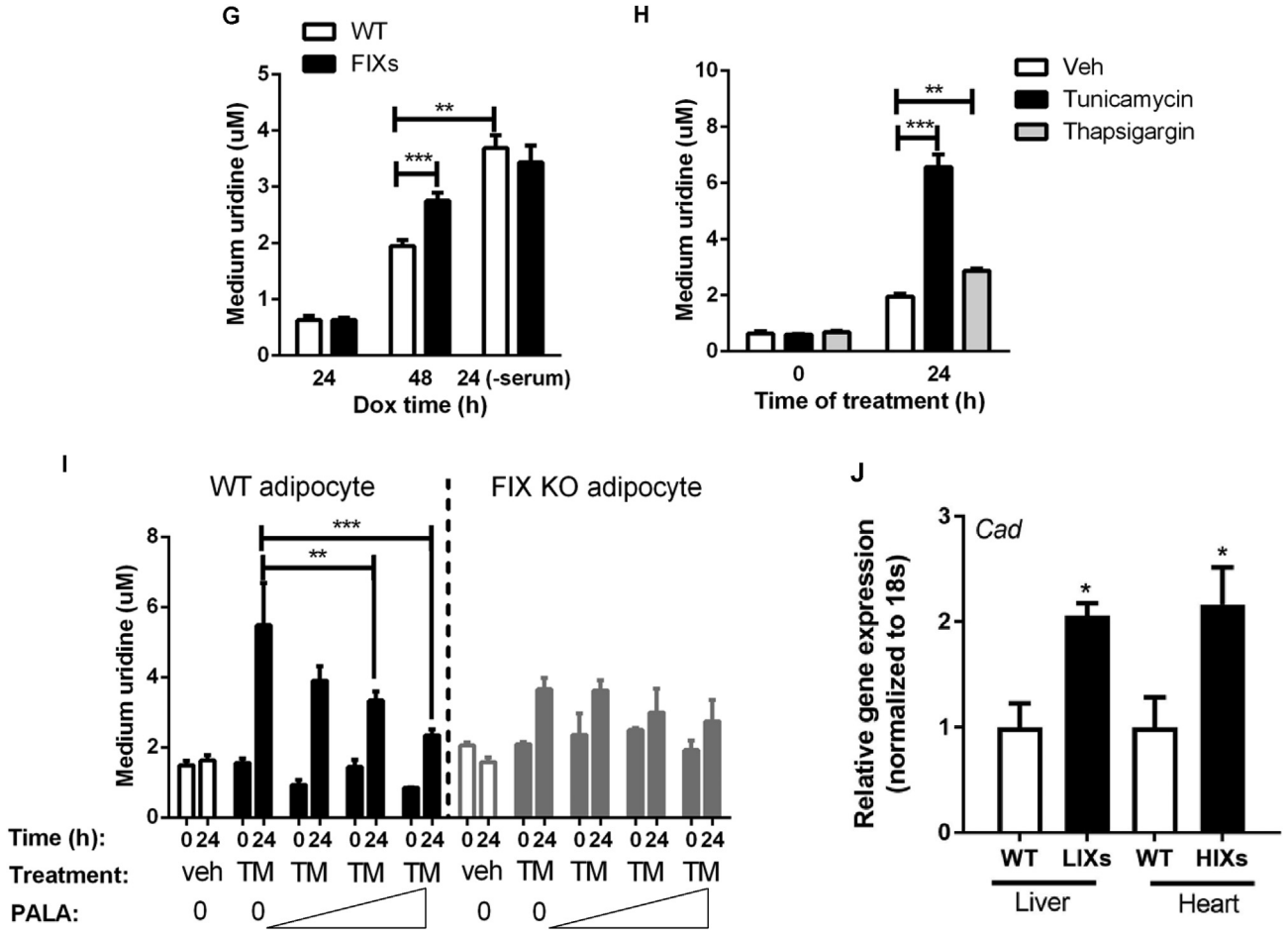

Figure 3: (*continued*).

supernatants for uridine measurements. According to the manufacturer's instruction, there is no uridine in DMEM-F12 medium, which was confirmed by our measurements (Figure 3F). Once the DMEM-F12 medium is supplemented with 10% fetal bovine serum, the uridine concentration reached 2 μM in the complete medium without cell culture, which is the baseline for the uridine levels in complete growth media (Figure 3F). To test the production of uridine in adipocytes as a function of Xbp1s, we supplemented Dox to complete medium and sampled the culture medium 24 h later for uridine measurements. We found that the uridine levels were reduced to 1 μM for both WT and FIXs adipocytes, suggesting a net consumption of uridine by the cells after the first 24 h Dox induction. The uridine concentrations then recovered to 2 μM after another 24 h for WT adipocytes, indicating a net release of uridine from adipocytes, which replenished the uridine in culture medium (Figure 3G). At this time point, the FIXs adipocytes increased the uridine concentrations in the culture medium to 2.8 μM, which is significantly higher than in WT adipocytes (Figure 3G). When WT and FIXs adipocytes were serum-starved during the second 24 h period, the uridine levels in medium were increased to 3.8 μM and 3.4 μM respectively (Figure 3G), both of which are significantly higher than that from cells cultured in complete medium, reflecting a stimulatory effect of serum starvation on uridine release from adipocytes. Serum starvation can cause ER stress, which might induce endogenous Xbp1s in adipocyte. To test if ER stress directly stimulates uridine synthesis and uridine release from adipocytes, we treated the differentiated adipocytes with tunicamycin or thapsigargin, compounds known to trigger ER stress acutely. We found that the uridine levels in the medium were elevated 3-fold and 1.5-fold by tunicamycin and thapsigargin (Figure 3H), respectively, indicating that ER stress can directly increase uridine release from adipocytes. The elevation caused by tunicamycin was suppressed dose-dependently by PALA, an inhibitor of *de novo* pyrimidine synthesis [19], indicating that ER stress-triggered uridine release is the result of *de novo* biosynthesis of uridine rather than catabolism of intracellular components (Figure 3I, **WT adipocyte**). Upon elimination of Xbp1 in the mature adipocyte, the suppression of uridine release by PALA was abolished (Figure 3I, **FIX KO adipocyte**), indicating that Xbp1s is necessary for pyrimidine synthesis in response to ER stress.

To test whether the activation of Cad by Xbp1s is a general mechanism, we analyzed the gene expression of *Cad* in mouse models in which we induced Xbp1s in cells other than adipocytes. In our previous studies, we have generated mouse models with inducible Xbp1s expression in hepatocytes in liver (LIXs mice) [11] and cardiomyocytes in the heart (HIXs mice) [20]. As expected, a tight correlation between Xbp1s and Cad expression was observed in each of these cell types (Figure 3J). This suggests that, while the fasting-induced increase in Xbp1s is unique to adipocytes, the ability of Xbp1s to induce Cad can occur in other cell types as well.

3.4. Adipocyte Xbp1s overexpression triggers fat mass loss but does not affect lifespan

Our data indicate that Xbp1s activation stimulates *de novo* pyrimidine synthesis in the adipocyte. This event leads to elevated plasma uridine levels, a physiological response to fasting seen in wild type mice as well [4]. Since lipolysis is also tightly associated with fasting, it is possible that part of the TG mobilized in adipocytes is consumed locally for the biosynthesis of pyrimidine, which is an anabolic process. This led us to examine whether chronic adipocyte-specific Xbp1s overexpression should increase TG mobilization, reducing fat mass over time. Indeed, FIXs mice started to reduce their bodyweight immediately upon switching to a Dox containing chow diet and reached a steady bodyweight by day 7 when the average bodyweight of FIXs mice was 4.7 g lighter than the bodyweight of WT mice, which were also exposed to Dox chow (Figure 4A). The bodyweight loss is mainly due to a reduction of fat mass as measured by MRI (Figure 4B), which is consistent with smaller WAT and BAT weights observed in the FIXs mice (Figure 4C). H&E staining shows a reduced adipocyte size in FIXs mice (Figure 4D). The rapid weight loss in FIXs mice, however, did not result in elevated fatty acid or ketone bodies in circulation upon fasting (Figure 4E), indicating the mobilized TG are consumed rapidly. The weight loss is also not triggered by insufficient insulin as the FIXs mice maintained their insulin levels comparable to WT after two weeks Dox induction (Figure 4F). Last but not least, chronic weight loss triggered by Xbp1s did not cause premature death. The lifespan of FIXs mice is comparable to WT mice on Dox chow, with a median survival time of 741 days for both genotypes (Figure 4G). While the life span is not increased in light of the reduced adiposity, less fibrosis and inflammation were observed in eWAT from 40-week old FIXs mice (Figure 4H).

3.5. Adipocyte Xbp1s overexpression prevents diet and leptin deficiency-induced obesity

To examine the potential of Xbp1s to prevent obesity, FIXs mice and age-matched control mice were switched to Dox containing high fat diet (HFD). The FIXs mice reduced their bodyweights from 37.4 g to 34.4 g seven days after the switch to DOX HFD diet, then continued reducing their bodyweight until they reached a plateau around 27.7 g two weeks later, which equals a ~20% reduction of bodyweight from the start point of DOX HFD exposure. This rapid weight loss is not due to toxicity or permanent damage to adipose tissue, as the FIXs mice increased their bodyweight promptly after the switch back to regular HFD (Figure 5A). Within one week, the FIXs mice increased their bodyweight to 33 g, a 95% recovery of the bodyweight from the starting point. It took 10 weeks for the FIXs mice to fully catch up with the WT mice on a regular HFD. After 112 days on regular HFD, the bodyweights of WT and FIXs mice reached 57.7 g and 53.8 g respectively, a point when the mice were 46 weeks old. We then switched the regular HFD back to Dox HFD to test if the obesity could be reversed. Again, the FIXs mice rapidly reduced their bodyweights, eventually reaching a plateau of 30 g, and maintained that bodyweight without a further reduction for another 15 weeks (Figure 5A). The overall adiposity in FIXs mice was significantly lower than in WT after switching to Dox HFD, reflecting the specific fat mass loss in FIXs mice (Figure 5B). Therefore, diet-induced obesity is both preventable and reversible in FIXs mice, regardless of age.

We also examined the ability of FIXs to drive fat mass loss in the *ob/ob* background, a model that develops obesity due to leptin deficiency. The switch to Dox chow efficiently slowed down the weight gain in *ob/ob* mice but, unlike FIXs mice in a wild type background, did not cause an actual net weight loss (Figure 5C), indicating that the effect of Xbp1s on the *ob/ob* mice is distinct from the FIXs mice challenged with a Dox HFD diet (Figure 5A). Nevertheless, the slower bodyweight gain observed in the FIXs, *ob/ob* mice was associated with a specific reduction in fat mass gain, as judged by a CT scan, reflecting a specific suppression of fat mass expansion (Figure 5D–E).

In contrast to gain-of-function of Xbp1s mutants, the FIX KO mice did not show a significant difference in bodyweight gain on Dox HFD (Figure 5F), indicating that Xbp1s is dispensable for fat mass expansion, consistent with the results reported for the constitutive adipocyte Xbp1s knockout [10]. However, after a 15-week regular HFD feeding, the bodyweight gain in the FIX KO mice trended higher than that in the control mice (Figure 5F), suggesting that Xbp1s may be required to prevent excessive expansion of fat mass once adiposity reaches an upper threshold. To test this, in a separate study, we waited for the mice to reach 69 weeks of age when their bodyweights were over 44 g prior to a switch to Dox HFD. Indeed, the FIX KO mice showed a significantly higher fat mass than the control mice (24.7 g vs 20.4 g) 4 weeks after the diet switch (Figure 5G), suggesting that adipocyte Xbp1 deficiency can cause higher adiposity in aged mice.

3.6. Adipocyte Xbp1s overexpression increases fatty acid oxidation and alters thermoregulation

A rapid fat mass loss suggests a net reduction of TG deposition in adipocytes. To pinpoint the underlying mechanism, we injected a trace amount of ^{3}H-triolein through the tail veins to measure both lipid uptake and fatty acid oxidation. Six days after the switch to Dox chow, the lipid uptake rates were comparable between FIXs and WT mice, whereas the fatty acid oxidation rates were significantly elevated in sWAT of FIXs mice (Figure 6A). Ninety days after the switch to Dox chow, the lipid uptake rates remained unchanged, whereas the fatty acid oxidation rates were increased in both sWAT and BAT in FIXs mice (Figure 6B). Thus, the fat mass loss in the FIXs mice does not result from a defect in fatty acid uptake, but rather from increased oxidation.

What is the mechanistic basis for the increased lipolysis in FIXs mice? We found that FIXs mice maintained their body temperature slightly but significantly lower than wild type mice (35.7 $\pm$ 0.12 °C vs 36.5 $\pm$ 0.18 °C) by day 10 of Dox exposure (Figure 6C), reflecting an altered thermoregulation, which, in turn, might drive fatty acid oxidation to defend body temperature. BAT is critical for heat production in response to cold exposure. BAT activation and browning of white adipocytes are well-known mechanisms for fat mass reduction in rodents. To determine whether BAT is involved in the weight loss observed in FIXs mice, we examined the transcriptional profile of multiple genes critical for BAT function. The FIXs mice had a drastic *downregulation* of the majority of the thermogenic genes in their BAT, including *Ucp1*, the classical BAT marker (Figure 6D), thereby excluding thermogenesis of BAT as a causative factor for weight loss. Furthermore, the expression of genes involved in adipocyte beiging did not increase in white adipose tissues from FIXs mice (Supplemental Fig. 2), indicating that beiging is not induced in FIXs mice and thus cannot be responsible for fat mass reduction. Food consumption and physical activity are two additional parameters affecting energy balance. In metabolic cage studies, we found no difference in food intake in FIXs mice (Figure 6E), whereas the ambulatory movements were just slightly increased (Figure 6F). This eliminates the possibility that the weight loss in FIXs mice cannot be explained on the basis of altered food intake or motility.

Since the classical mechanisms known for weight loss are not applicable, we looked for the relevance of the uridine biosynthetic pathway to impose weight loss in FIXs mice. Uridine is known to trigger hypothermia in mice potentially through vessel dilation [21]. FIXs mice

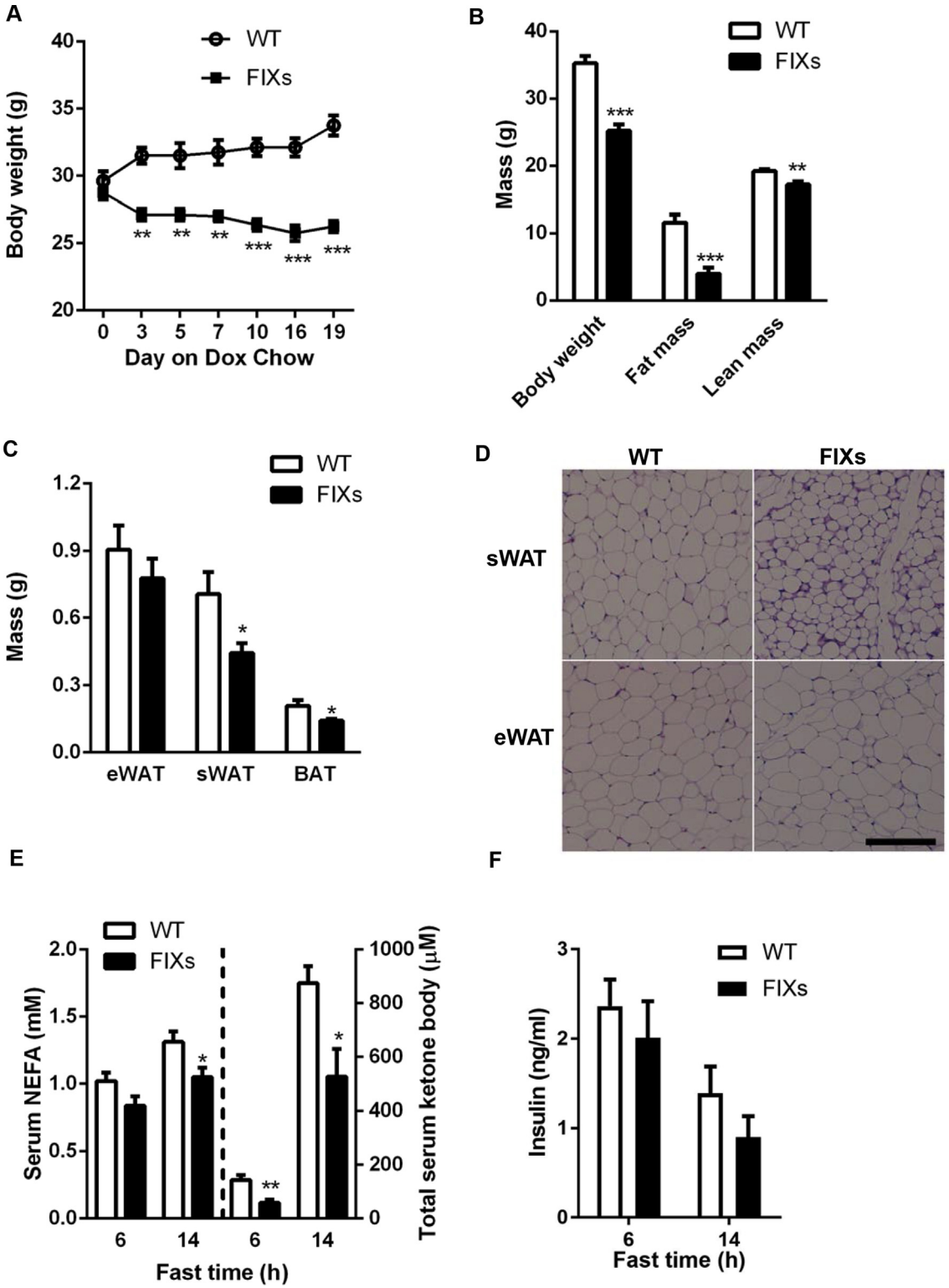

Figure 4: Adipocyte Xbp1s overexpression reduces fat mass but not lifespan. (A) Adipocyte Xbp1s overexpression led to reduction of bodyweight (n = 4). (B) Overexpression of Xbp1s in adipocytes reduced fat mass (n = 6). (C) Overexpression of Xbp1s led to reduction of fat depot mass (n = 9–10). (D) Representative H&E staining image of WATs. Scale bar, 200 μM. (E) Overexpression of Xbp1s in adipocytes caused lower levels of free fatty acids and ketone bodies under fasted condition (n = 6). (F) Overexpression of Xbp1s in adipocytes did not change insulin levels under fasted condition (n = 6). (G) Lifespan of male mice on Dox chow (n = 34 for WT, n = 24 for FIXs). (H) Representative H&E staining image of WATs from 40 weeks old male mice that were maintained on Dox chow from 7 weeks of age. Scale bar 100 μM, Data were analyzed with two-tailed Student *t* test. *, $p < 0.05$; **, $p < 0.01$, ***, $p < 0.001$. Error bars denote SEM.

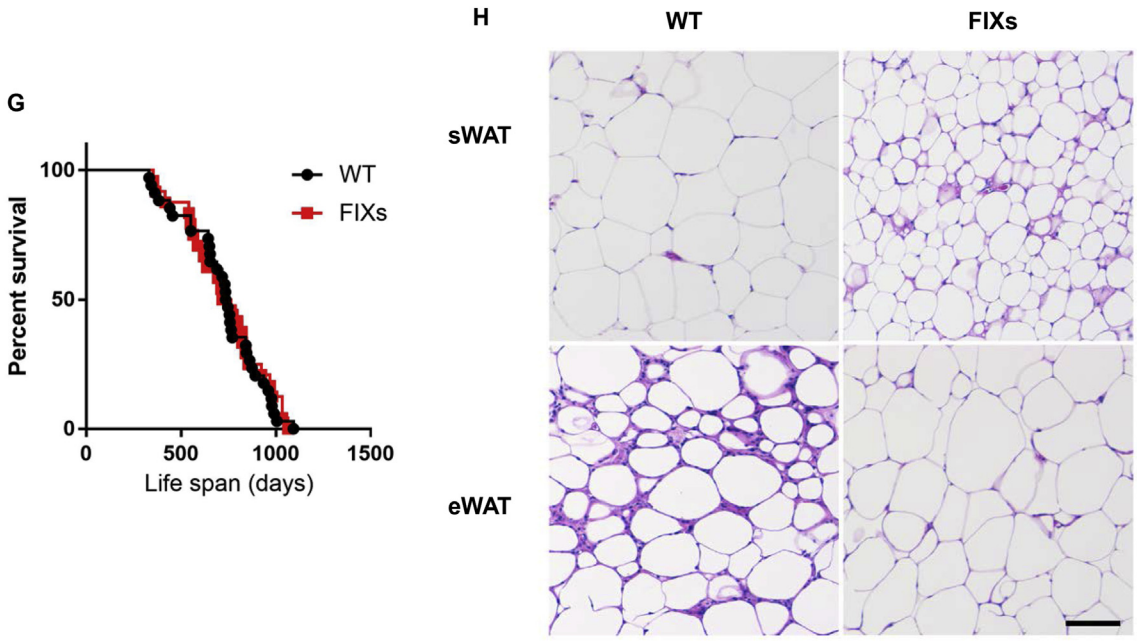

Figure 4: (*continued*).

have constitutively elevated plasma uridine levels (Figure 2C). It is possible that the lower body temperature is the result of elevated plasma uridine. When uridine synthesis is uncoupled from regulation of fasting/refeeding as observed in the FIXs mice, the excessive production of uridine in adipocytes could be part of a "futile cycle" that consumes energy for the biosynthesis just to dispose of excess uridine through the bile and other mechanisms. Therefore, the TGs in adipocytes are mobilized to support uridine synthesis locally. However, an issue with this proposed mechanism is that a lower body temperature usually reflects a lower rate of basal metabolism. Lower basal metabolic rate should lead to lower heat production, thereby lower energy expenditure and increased obesity, as typically observed in *ob/ob* mice. To clarify this, we performed metabolic cage studies to measure basal metabolic rates. Within 10 days after the switch to Dox chow, FIXs mice displayed significantly higher rates of O_2 consumption and CO_2 release under fed, fasted and refed conditions (Figure 6G—H), indicating an increased metabolic rate in the FIXs mice compared to WT mice. The heat production in FIXs mice was significantly higher than in WT mice under all conditions tested (Figure 6I), confirming that the slightly lower core body temperature is due to enhanced heat release instead of impaired heat production. Therefore, heat release is increased in FIXs mice by means of an enhanced metabolic rate and to a lesser extent, also through elevated physical activity. As a result, there is a net fat mass loss over time.

3.7. Fat mass loss triggered by Xbp1s depends on pyrimidine synthesis

Based on the analysis above, we believe that uridine biosynthesis is critical for the Xbp1s-mediated fat mass reduction. To test whether the increased uridine production in adipocytes is the actual cause for fat mass loss, we induced ectopic Xbp1s expression in mice harboring an adipocyte-specific Cad knockout (Figure 7A). The CAD KO mRNA which has exon 3 deleted can only be detected in the Cad KO genotype, not in Cad WT mice (Figure 7B). Consistent with the gene expression data, full-length CAD protein levels in isolated floated adipocytes are significantly reduced in the Cad KO mice (Figure 7C). As expected, the FIXs mice reduced their bodyweight after the switch to the Dox chow diet, whereas the FIXs mice in the adipocyte-specific Cad KO continued to increase their bodyweight, though not to the same extent as the wildtype mice (Figure 7D). Therefore, the CAD knockout partially reverses the effect of Xbp1s in the adipocyte. Mice lacking Cad alone did not show a significant difference to wild type mice with respect to their bodyweight gain, indicating the partial elimination of CAD alone has no deleterious effects on growth (Figure 7D). When examined by H&E staining, the size of adipocytes was reduced in FIXs mice in sWAT, eWAT and BAT. However, this change was fully reversed in FIXs/Cad KO mice (Figure 7E). The Cad KO mice without ectopic Xbp1s displayed a moderate size reduction of adipocytes in sWAT, but no differences in eWAT or BAT compared to wild type (Figure 7E). We then verified that the difference in growth and adipocyte morphology between FIXs and FIXs/Cad KO mice is not due to differential Xbp1s induction, because the gene expression of Xbp1s was elevated to the same extent in eWAT and sWAT of the different genotypes (Figure 7F). The induction of Xbp1s expression in BAT from FIXs/Cad KO mice was less than in FIXs mice, indicating a potential negative feedback of Cad deletion to Xbp1s expression (Figure 7F). The tissue uridine content was increased in adipose tissue from FIXs mice but not FIXs/Cad KO mice (Figure 7G), confirming the activation of pyrimidine synthesis by Xbp1s is abolished by CAD ablation. Therefore, *de novo* uridine biosynthesis in adipocytes is required for weight loss driven by adipocyte Xbp1s overexpression. We have recently reported that both genetic and diet-induced obese mice have altered plasma uridine homeostasis in response to fasting/refeeding, indicating that obesity is associated with disrupted plasma uridine homeostasis [4]. However, in contrast to FIXs mice that show elevated plasma uridine and a reduction in weight, *ob/ob* mice display obesity despite elevated plasma uridine [4]. Therefore, an elevation of plasma uridine does not seem to correlate with a reduction of fat mass. The difference in adiposity between *ob/ob* and FIX mice lies in the source of plasma uridine. To demonstrate this, we measured the uridine content of tissue under these two different conditions. The

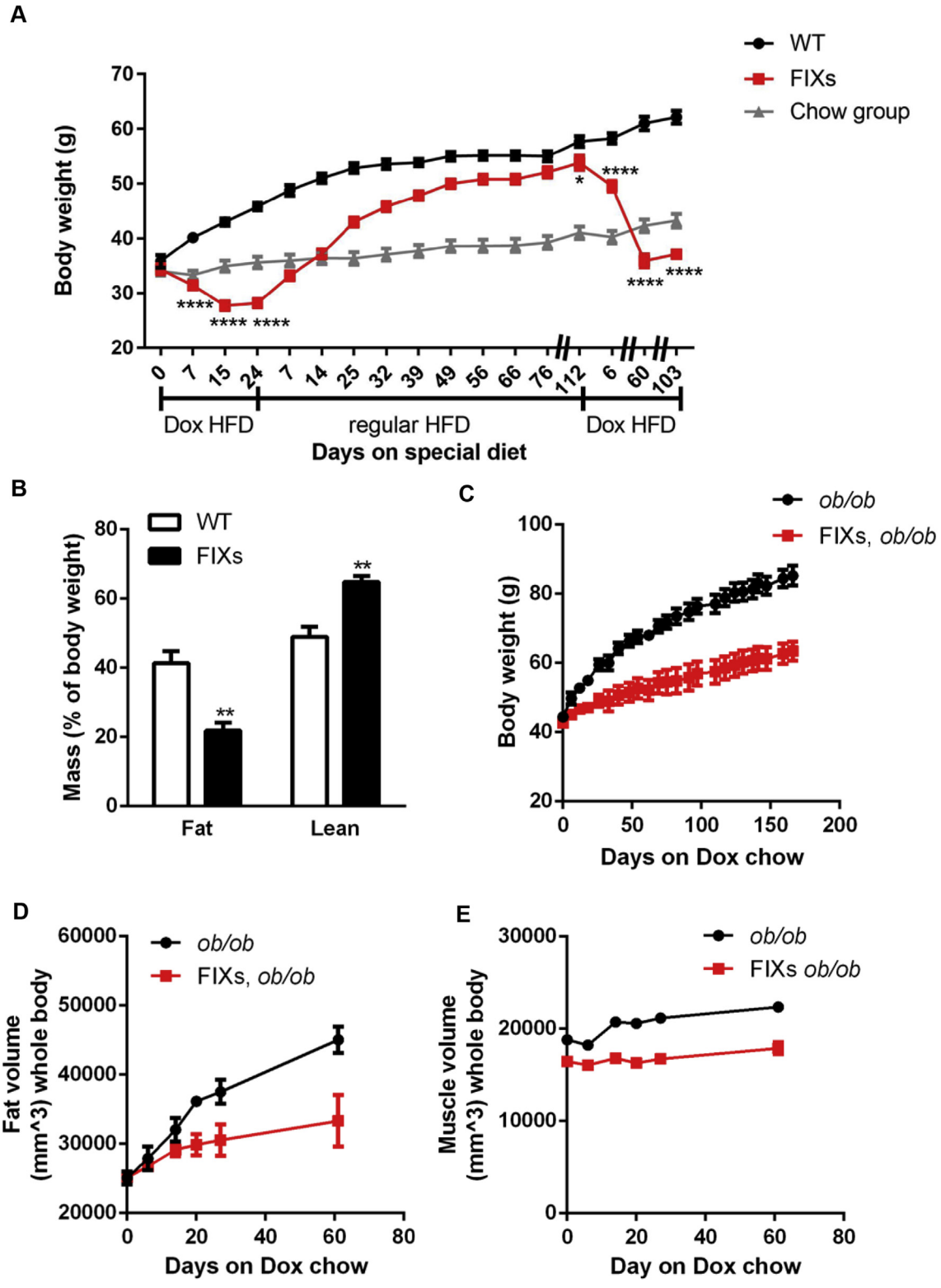

Figure 5: Adipocyte Xbp1s overexpression protects mice from obesity. (A) Mice were maintained on regular chow until 27–32 weeks old to start Dox HFD feeding. Bodyweight of FIXs mice was reduced by Dox HFD and increased by regular HFD, which was not observed in WT mice (n = 7–11). The Chow group were age-matched WT mice that were maintained on regular chow during the course of study (n = 15). (B) Fat mass and lean mass of mice were determined by MRI after 100 days on HFD Dox (n = 6). (C)–(E) Mice on *ob/ob* background were maintained on regular chow until 11 weeks old to start Dox Chow feeding. Bodyweight mice were monitored for 166 days on Dox. Fat volume and muscle volume of mice were measured by CT scan at indicated time after switch to Dox chow (n = 3). (F) Mice were maintained on regular chow until 27–32 weeks old to start Dox HFD feeding. Bodyweight of mice was monitored after switch to Dox HFD, back to regular HFD and then Dox HFD again (n = 6). The Chow group were age-matched WT mice shared in the study of Figure 5A. (G) Mice were maintained on regular chow until 69 weeks old to start Dox HFD. Fat mass and lean mass of mice were determined by MRI 4 weeks after switch to HFD Dox (n = 8). Data were analyzed with two-tailed Student *t* test. *, $p < 0.05$, **, $p < 0.01$, ***, $p < 0.001$, ****, $p < 0.0001$. Error bars denote SEM.

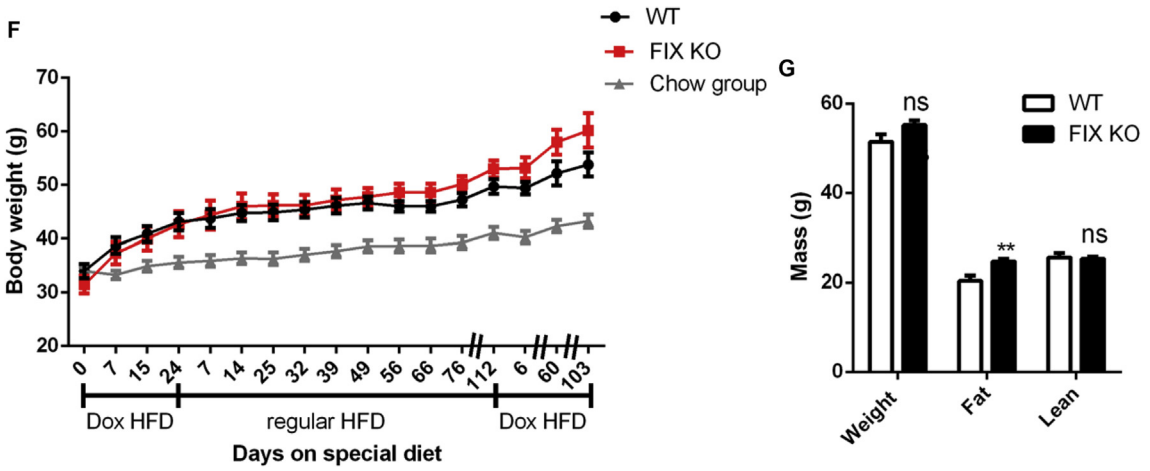

Figure 5: (*continued*).

sWAT from *ob/ob* mice has significantly less uridine than in lean littermates, whereas the eWAT and liver uridine content are not different (Figure 7H). Similarly, the sWAT from *db/db* mice has significantly less uridine than WT, whereas eWAT, BAT, and liver uridine content are not different (Figure 7I). In contrast, all three fat depots from 8 week HFD fed mice show similar uridine content to the tissues isolated from the chow group (Figure 7J). We then compared tissue uridine content from wild type mice under fed and fasted condition. The sWAT and BAT from fasted mice has significantly higher amounts of uridine than in tissues isolated from fed mice, whereas eWAT uridine content is not different (Figure 7K). Importantly, the liver from fasted mice has less uridine than in fed mice (Figure 7K), confirming that uridine biosynthesis in liver is reduced by fasting [4]. Together our data demonstrates that an elevation of tissue uridine by fasting only occurs in sWAT and BAT, but not in the liver, indicating that the elevation of uridine in sWAT is unlikely due to a generic increased uptake of uridine from plasma. While HFD-induced obesity is not associated with an elevation of uridine in adipose tissue, leptin deficiency is associated with a significant reduction of uridine in sWAT, but not liver or other fat depots. This suggests that uridine biosynthesis is not altered or increased in adipocytes in obese mice. When lipolysis is triggered in mice by treatment with streptozotocin (STZ); however, the strong lipolytic component does not lead to an elevation in plasma uridine. Rather, the plasma uridine levels drop and so does the tissue uridine content in BAT [4]. Therefore, the elevated uridine production in adipose tissues by Xbp1s overexpression is the result of accelerated uridine biosynthesis rather than a direct result of lipolysis. Lipolysis is therefore required, but not sufficient, for uridine production in the adipocyte.

4. DISCUSSION

4.1. De novo uridine synthesis is regulated by Xbp1s

Xbp1s, conventionally known as an UPR transducer that is induced by ER stress, is critical for ER homeostasis through activating the transcriptional program of an array of target genes [9]. One of the established roles for Xbp1s in *alleviating* ER stress is to enhance phospholipid synthesis, a response conserved from yeast to mammals [22]. The potential target gene(s) that mediate this action remain unknown. Pyrimidine is required for phospholipid biosynthesis through pyrimidine conjugation to lipid and choline. CAD is the first and rate-limiting enzyme for *de novo* pyrimidine synthesis. In 2015, the first observed pathological mutations of CAD were reported in a four-year-old individual [23]. This study showed glycosylation precursors were decreased in the patient, indicating *de novo* pyrimidine biosynthesis is critical for protein glycosylation in mammals and hence, ER homeostasis. However, it was not known whether the ER stress response can directly regulate pyrimidine synthesis. Our past studies have revealed that Xbp1s plays a critical role in anabolic reactions and the regulation of signaling through two new transcriptional target genes, *GalE* and *Gfap1* [11,20]. Both enzymes use pyrimidine-conjugated sugars to generate modifications on proteins. Thus, our studies identifying *Cad* as a target gene of Xbp1s is consistent with previous observations and offer a molecular mechanism for ER stress regulated pyrimidine synthesis. Verified in multiple, distinct inducible mouse models, transcriptional activation of *Cad* associates with Xbp1s in adipocytes, hepatocytes, and cardiomyocytes, indicating the activation of *Cad* by Xbp1s is a general mechanism conserved in multiple cell types. Recent studies have highlighted the role of Xbp1s in the development of several types of secretory cells [25] as well as tumors [26]. Cad expression is also augmented in tumors and suppressed by apoptosis [27,28]. Considering that *Cad* is the first and rate-limiting enzyme for *de novo* pyrimidine synthesis and pivotal for cell proliferation, the activation of *Cad* by Xbp1s provides additional insight for the physiology of ER stress involvement in cell growth ranging from normal cell turnover during development and immune response to the pathological cell proliferation in the context of tumors and cancer.

4.2. Adipocyte Xbp1s is induced by lipolysis, and stimulates uridine production

It remains unknown how Xbp1s induction is regulated in adipocytes. We found Xbp1s induction in adipose tissue is associated with lipolysis, suggesting lipolytic stimuli might be involved in the induction of Xbp1s. Since the constitutive adipocyte-specific Xbp1s knockout mice do not show a difference in adiposity [10] (a phenotype which is reproduced in our inducible FIX KO mice), we conclude that Xbp1s induction is not absolutely required for lipolysis. Given the data we provide here, a likely role of Xbp1s in adipocytes *in vivo* is to stimulate uridine synthesis such that plasma uridine levels can be increased. This is consistent with our recent study that reveals the physiological relevance of plasma uridine elevation to temperature control in response to fasting [4]. In addition to fasting, this Xbp1s-Cad axis mediated pyrimidine synthesis activity also affects other biological

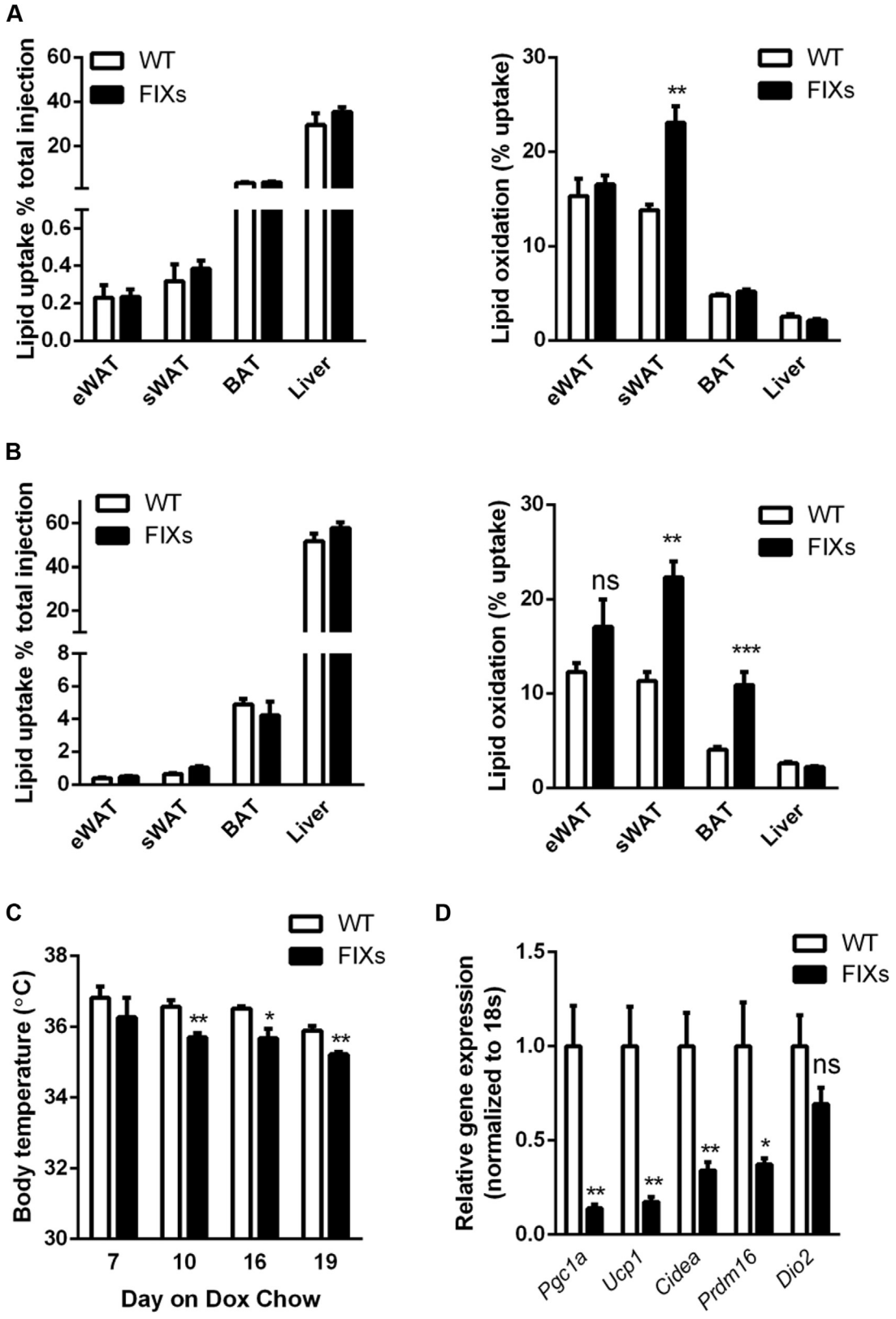

Figure 6: Adipocyte Xbp1s overexpression increases fatty acid oxidation and heat production. (A) Xbp1s overexpression in adipocytes for 6 days increased fatty acid oxidation without affecting lipid uptake (n = 6). (B) Xbp1s induction in adipocytes for 90 days increased fatty acid oxidation in multiple fat depots without affecting lipid uptake (n = 6). (C) Body temperature was monitored after mice were switched to Dox chow (n = 4). (D) Xbp1s overexpression in adipocytes for 6 days reduced expression of most thermogenic genes in BAT (n = 8). (E)–(I) Metabolic cage studies were conducted to measure food intake, physical activities, O_2 consumption, CO_2 release, and heat production in mice. A 24 h fast was performed from 12 AM to 12 AM during the study (n = 5). Data were analyzed with two-tailed Student *t* test. *, $p < 0.05$, **, $p < 0.01$, ***, $p < 0.001$. ns, not significant. Error bars denote SEM.

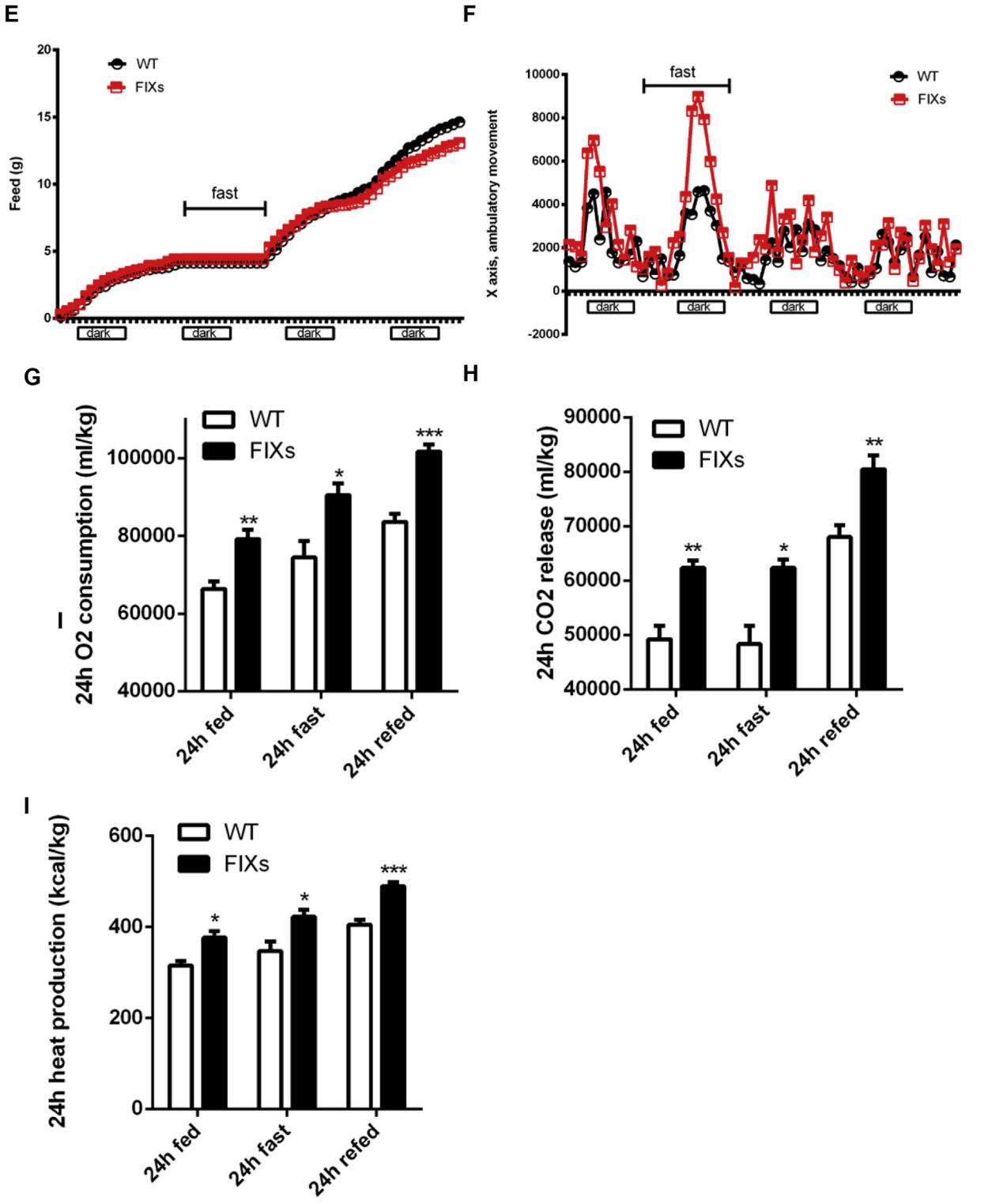

Figure 6: (*continued*).

processes, such as lactation and tumorigenesis. Xbp1s is activated in adipocytes during lactation and is necessary for lipolysis during lactation [10]. Uridine and its derivatives cytidine and thymidine are not only required for mammary epithelial cell proliferation during lactation but also are highly enriched in breast milk [29]. Thus, our study suggests a potential link between lipolysis and uridine production during lactation, which likely explains why the adipocyte-specific Xbp1s knock out females display reduced milk production [10]. CAD is activated in tumor cells [27], and this enhanced capacity for pyrimidine biosynthesis is believed to provide the uridine nucleotides that

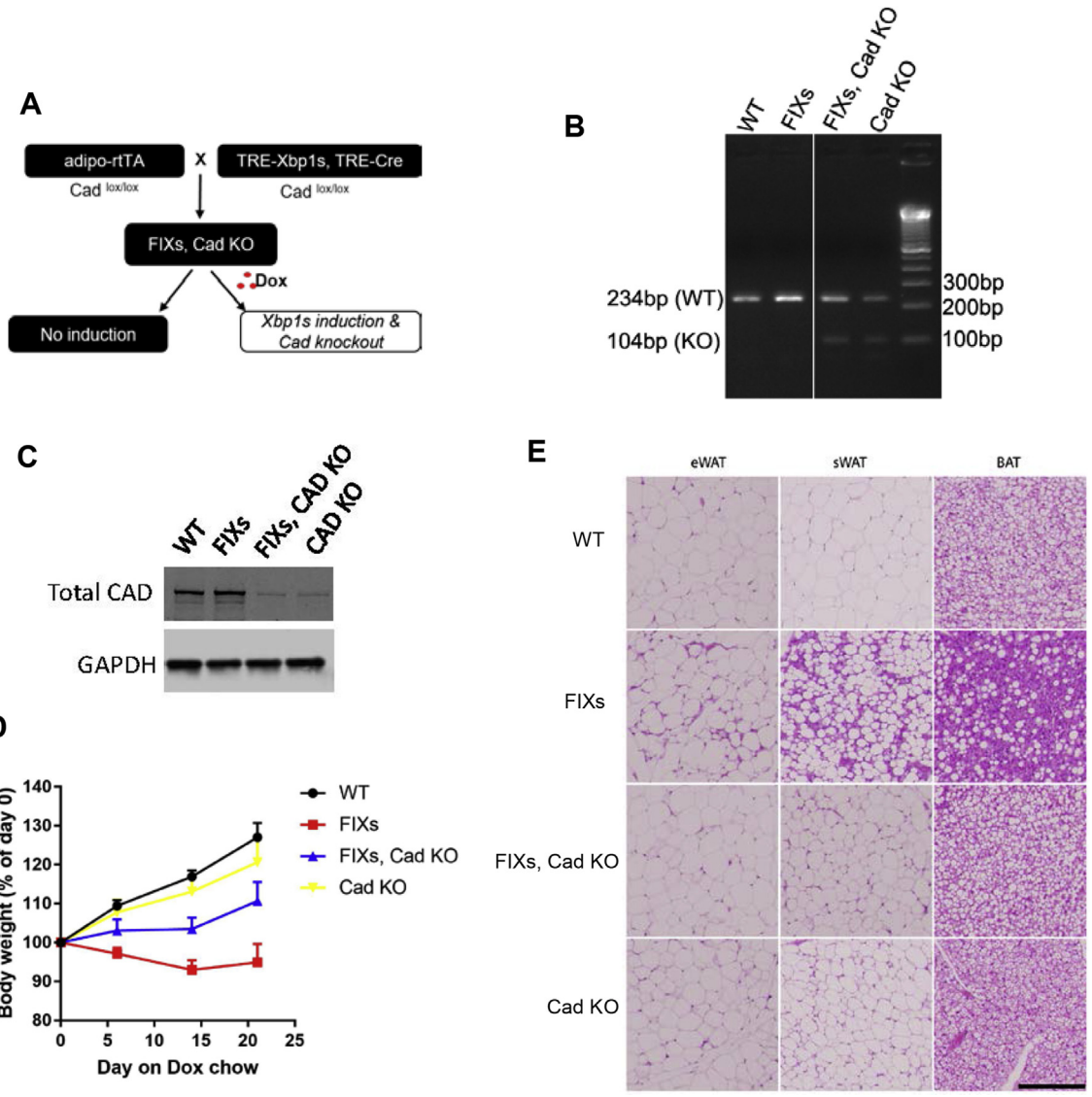

Figure 7: Adipocyte Cad knockout prevents pyrimidine synthesis and weight loss triggered by Xbp1s overexpression. (A) Strategy for the generation of mouse model for inducible adipocyte Xbp1s overexpression and Cad knockout (FIXs, Cad KO). (B) Representative gel image of PCR products of CAD from BAT derived cDNA. Exon 3 of CAD, which contains 130 nucleotides, is flanked by two loxP sites. The removal of exon 3 in CAD gene produces a CAD mutant transcript which can generate a 104 bp PCR product amplified from the cDNA with specifically designed primer set (Supplemental Table 1). (C) Representative western blot image of full-length CAD protein in adipocytes isolated from sWAT. GAPDH was blotted as loading control. (D) Bodyweight of mice prior to and post switch to Dox chow (WT, n = 9; FIXs, n = 7; FIXs, Cad KO, n = 6; Cad KO, n = 5). (E) Representative H&E staining image of adipose tissues from mice. Scale bar, 200 μM. (F) Gene expression of Xbp1s in fat depots (n = 3–4 each group). (G) Uridine concentrations in fat depots and liver (n = 3–4). Statistical analysis was performed for each tissue type using WT mice as base line if not specified. (H) Uridine concentrations in liver and fat depots from WT and *ob/ob* mice that were 19–23 weeks old on chow (n = 5). The *ob/ob* mice lack visible BAT at the time of harvest. (I) Uridine concentrations in liver and fat depots from WT and *db/db* mice that were 28–31 weeks old on chow (n = 5). (J) Uridine concentrations in liver and fat depots from WT male mice that were 19–21 weeks old and on HFD for 8 weeks (n = 4). (K) Uridine concentrations in liver and fat depots from WT male mice that were 26–31 weeks old and on Dox chow from 8 weeks of age (n = 5–6). Data were analyzed with two-tailed Student *t* test. *, $p < 0.05$, **, $p < 0.01$. ns, not significant. Error bars denote SEM.

are required for rapid cell growth [30]. ER stress and Xbp1s are also found to be increased in tumor lesions and are critical for tumor growth [26,31]. Our data indicate the activation of *Cad* under these conditions might be a direct result of ER stress, providing a direct connection of ER stress and cancer metabolism.

4.3. Adipocyte Xbp1s overexpression reduces obesity by stimulating uridine production

Obesity is a major public health issue and a cause for several chronic diseases. Finding ways to enhance lipolysis and fatty acid oxidation is critical for the identification of new therapeutic areas. Our results indicate that adipocyte Xbp1s overexpression can efficiently drive fat mass loss. Since Xbp1s is dispensable for adipogenesis [10], and our inducible FIXs mice are under the control of the adiponectin promoter, an adipocyte marker expressed only in mature adipocytes, the fat mass loss in FIXs mice is not due to a defect in adipogenesis. This is further supported by our observation that the FIXs mice can rapidly recover their bodyweight upon switching back to a regular diet lacking doxycycline. Intriguingly, the loss of fat mass is not the result from altered food intake or motility, and neither is it mediated through

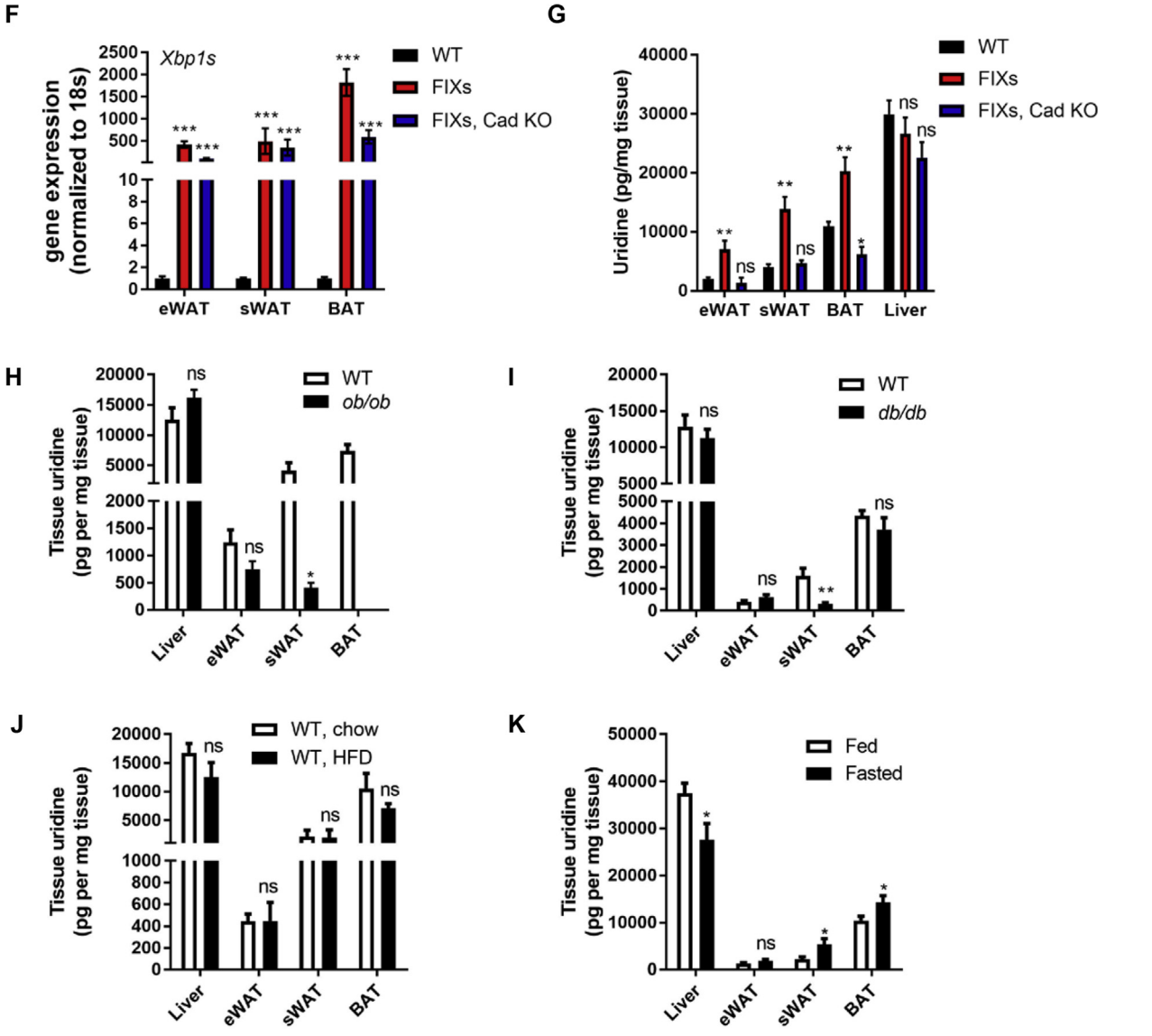

Figure 7: (*continued*).

adipocyte browning and/or beiging. Our results, however, indicate the weight loss is due to chronic uridine production within adipocytes. We found induction of Xbp1s with a lower dose of Dox (200 mg/kg) does not cause significant weight loss in FIXs mice, indicating a dose-dependent action of Xbp1s in activating pyrimidine synthesis to achieve a systemic effect on energy homeostasis. Therefore, a moderate elevation of adipocyte Xbp1s in rodents is not expected to cause efficient weight loss, which has been reported by Qi and colleagues [32]. Of importance is the fact that the induction of Xbp1s leads to a rapid decrease of TG in adipocytes, manifest in a profound weight loss, however without the development of lipodystrophy. These FIXs mice do not seem to suffer from any pathological side effects and, in fact, show survival rates at least as high as WT mice. Thus, activation of uridine production from adipocytes can be viewed as a possible therapeutic avenue for obesity. Importantly, lipolysis is frequently triggered by insulin resistance in adipocytes. The fat mass loss in FIXs mice, however, is completely different from insulin resistance- or streptozotocin (STZ)-triggered lipolysis that is mediated by a lack of insulin signaling. STZ treatment can lead to complete loss of WATs and a decrease of uridine in plasma and bile. The BAT from STZ treated mice, the only remaining dissectible fat depot after prolonged hypoinsulinemia, has its uridine content reduced by 50%, reflecting a severe reduction in *de novo* uridine production induced by STZ [4]. The accumulation of uridine in adipose tissue observed in FIXs mice, therefore, is not due to insulin resistance/lack of insulin signaling. In fact, the FIXs mice maintain their fed insulin concentrations similar to control mice. The rapid reduction of adipocyte TG therefore reflects lipolysis but is not primarily driven by lipolysis alone. Lipolysis, while necessary, is insufficient to observe the uridine biosynthetic phenotype. Rather, the efficacy of Xbp1s in stimulating uridine biosynthesis is found to be higher in BAT and sWAT relative to eWAT, reflected by a more pronounced fat mass reduction in BAT and sWAT compared to eWAT. Meanwhile, there appears to be a higher rate of infiltration of immune cells in sWAT of FIXs mice. This may reflect a higher degree of local inflammation in adipose tissue of Xbp1s overexpressing mice. Together, this may be the reason why the overall reduction in fat mass

does not lead to a beneficial lifespan extension in FIXs mice. At this point, we do not understand why the eWAT remains more resistant to Xbp1s-mediated stimulation of uridine biosynthesis. Given that uridine biosynthesis is a process orchestrated at multiple levels, the supply of substrates, the ATP production, and the functionality of mitochondria (harboring DHODH, the second enzyme for *de novo* uridine biosynthesis) might all be different in eWAT, limiting the efficiency of uridine biosynthesis relative to BAT and sWAT. Chronic ER stress can impact on lipogenesis [33], so decreased lipogenesis may also contribute to fat mass loss upon chronic overexpression of Xbp1s. This would be consistent with the finding that CAD knockout does not completely neutralize the weight loss phenotype seen upon Xbp1s overexpression.

4.4. Adipocyte Xbp1s overexpression alters energy homeostasis through plasma uridine elevation

How does chronic uridine production in adipocytes lead to weight loss systemically? It is known that uridine can stimulate a drop in body temperature, potentially through vessel dilation [21]. Thus, the lower body temperature in FIXs mice suggests more heat is lost from the system, which is consistent with the metabolic cage studies showing that the heat release from FIXs mice is significantly higher than that seen for wild type mice. This indicates that under physiological conditions, in response to fasting (associated with enhanced lipolysis), plasma uridine elevation is triggered to facilitate a drop in body temperature. The slightly lower body temperature leads to a reduction in energy consumption, serving as an adaptive response to fasting and starvation. Once the body temperature is lowered and metabolic rates are reduced, uridine production is likely to be reduced too, such that torpor or hypothermia is prevented. However, in the FIXs mouse, uridine synthesis is uncoupled from this feedback regulation. The elevated plasma uridine leads to a higher heat loss under fed conditions. In response to this chronic heat loss, oxygen consumption and lipid oxidation are increased with the aim of producing more heat to defend body temperature. The slightly lower body temperature observed in the FIXs mice is the net result of higher heat loss and higher heat production. Consistent with this physiology, the metabolic cage studies show a higher O_2 consumption rate and CO_2 release with no increase in food intake. The mechanistic basis for the increased heat production in these FIXs mice is not entirely clear. Our data indicates fatty acid oxidation is increased in sWAT and BAT. It is therefore possible that fatty acid oxidation is also increased in other tissues, such as skeletal muscle, and therefore heat produced by muscle through shivering may be a mechanism of increased heat production seen in these mice. Also, maintaining normal body temperature in the FIXs mice may also be energetically more expensive in light of the reduced adiposity with reduced capacity to insulate. It is possible that the reduction of triglyceride content in subcutaneous white adipose tissues in FIXs mice may also lead to reduced lipid content in dermal adipose tissue, which leads to a further increase in heat loss. Although the FIXs mouse under study is an artificial model with a deregulation of Xbp1s, the effect on fat mass loss suggests a potential mechanism for cachexia-driven lipolysis. Lipoatrophy also occurs in HIV-associated lipodystrophy, and the uridine levels in the fat from HIV-infected patients are found to be significantly elevated [34]. Our data strongly suggest that lipolysis could be enhanced by uridine synthesis and subsequent release at the level of adipocytes. While speculative at this point, it may be that a high demand for adipose tissue-derived uridine biosynthesis serves as the key driver for cancer cachexia-induced lipolysis and ultimate weight loss.

In summary, we describe a molecular mechanism for Xbp1s-regulated *de novo* pyrimidine synthesis and dissect the impact of chronic adipocyte Xbp1s induction on lipolysis and uridine biosynthesis. The gain-of-function mouse model used in our studies demonstrates a potent protection from obesity through adipocyte Xbp1s activation, which is likely driven by excessive heat loss through elevated plasma uridine. Our data suggest a direct regulatory role of ER stress in pyrimidine metabolism and reveals that activation of uridine synthesis in adipocytes is a potential mechanism to trigger TG mobilization.

AUTHOR CONTRIBUTIONS

YD conceived the study, designed and performed the experiments, analyzed data, and wrote the manuscript. ZVW performed the fatty acid oxidation and immunoblotting assays. RG performed uridine measurement. YZ performed the study using adipocyte differentiated from SVF. AA performed mouse CT scan and fat volume quantification. CZ and XW helped with sample collection and qPCR assay. PI helped with the cachexia mouse study. MS and RG helped with adipocyte browning and beiging analysis. ZZ helped with adipocyte isolation from fat tissue. JDH and JAH contributed to the discussion. PES conceived the study and wrote the manuscript.

ACKNOWLEDGEMENTS

We thank Wei Tan (Division of Cardiology, UT Southwestern Medical Center) for excellent technical assistance. We thank Q. Liang and J. Brabander for the synthesis of PALA (Department of Biochemistry and Simmons Comprehensive Cancer Center, UT Southwestern Medical Center). This work was supported in part by a postdoctoral fellowship from the American Diabetes Association (7-08-MN-53) (to YD), a Scientist Development Grant from the American Heart Association (14SDG18440002) (to ZVW), NIH grants R01-DK55758 and R01-DK099110 and P01-AG051459 (PES), and P01-DK088761 (PES, JKE, JDH). PES was also supported by an unrestricted grant from the Novo Nordisk Research Foundation. JAH was supported by grants from the National Institutes of Health (HL-120732, HL-128215, HL-126012), the American Heart Association (14SFRN20510023; 14SFRN20670003), the Fondation Leducq (11CVD04), and the Cancer Prevention and Research Institute of Texas (RP110486P3).

APPENDIX A. SUPPLEMENTARY DATA

Supplementary data related to this article can be found at https://doi.org/10.1016/j.molmet.2018.02.013.

CONFLICT OF INTEREST

The authors declare no conflicts of interest.

REFERENCES

[1] Levine, R.L., Hoogenraad, N.J., Kretchmer, N., 1974. A review: biological and clinical aspects of pyrimidine metabolism. Pediatric Research 8(7):724—734.
[2] Yamamoto, T., Koyama, H., Kurajoh, M., Shoji, T., Tsutsumi, Z., Moriwaki, Y., 2011. Biochemistry of uridine in plasma. Clinica Chimica Acta 412(19—20): 1712—1724.
[3] Gasser, T., Moyer, J.D., Handschumacher, R.E., 1981. Novel single-pass exchange of circulating uridine in rat liver. Science 213(4509):777—778.
[4] Deng, Y., Wang, Z.V., Gordillo, R., An, Y., Zhang, C., Liang, Q., et al., 2017. An adipo-biliary-uridine axis that regulates energy homeostasis. Science 355(6330).
[5] Attie, A.D., Scherer, P.E., 2009. Adipocyte metabolism and obesity. The Journal of Lipid Research 50(Suppl):S395—S399.
[6] Zechner, R., Zimmermann, R., Eichmann, T.O., Kohlwein, S.D., Haemmerle, G., Lass, A., et al., 2012. FAT SIGNALS—lipases and lipolysis in lipid metabolism and signaling. Cell Metabolism 15(3):279—291.

[7] Hotamisligil, G.S., 2010. Endoplasmic reticulum stress and the inflammatory basis of metabolic disease. Cell 140(6):900–917.

[8] Bogdanovic, E., Kraus, N., Patsouris, D., Diao, L., Wang, V., Abdullahi, A., et al., 2015. Endoplasmic reticulum stress in adipose tissue augments lipolysis. Journal of Cellular and Molecular Medicine 19(1):82–91.

[9] Ron, D., Walter, P., 2007. Signal integration in the endoplasmic reticulum unfolded protein response. Nature Reviews Molecular Cell Biology 8(7):519–529.

[10] Gregor, M.F., Misch, E.S., Yang, L., Hummasti, S., Inouye, K.E., Lee, A.H., et al., 2013. The role of adipocyte XBP1 in metabolic regulation during lactation. Cell Reports 3(5):1430–1439.

[11] Deng, Y., Wang, Z.V., Tao, C., Gao, N., Holland, W.L., Ferdous, A., et al., 2013. The Xbp1s/GalE axis links ER stress to postprandial hepatic metabolism. Journal of Clinical Investigation 123(1):455–468.

[12] (a) Sun, K., Wernstedt Asterholm, I., Kusminski, C.M., Bueno, A.C., Wang, Z.V., Pollard, J.W., et al., 2012. Dichotomous effects of VEGF-A on adipose tissue dysfunction. Proceedings of the National Academy of Sciences of the United States of America 109(15):5874–5879.
(b) Wang, Z.V., Deng, Y., Wang, Q.A., Sun, K., Scherer, P.E., 2010. Identification and characterization of a promoter cassette conferring adipocyte-specific gene expression. Endocrinology 151(6):2933–2939.

[13] Perl, A.K., Wert, S.E., Nagy, A., Lobe, C.G., Whitsett, J.A., 2002. Early restriction of peripheral and proximal cell lineages during formation of the lung. Proceedings of the National Academy of Sciences of the United States of America 99(16):10482–10487.

[14] Lee, A.H., Scapa, E.F., Cohen, D.E., Glimcher, L.H., 2008. Regulation of hepatic lipogenesis by the transcription factor XBP1. Science 320(5882):1492–1496.

[15] Laplante, M., Festuccia, W.T., Soucy, G., Blanchard, P.G., Renaud, A., Berger, J.P., et al., 2009. Tissue-specific postprandial clearance is the major determinant of PPARgamma-induced triglyceride lowering in the rat. American Journal of Physiology - Regulatory, Integrative and Comparative Physiology 296(1):R57–R66.

[16] Shao, M., Ishibashi, J., Kusminski, C.M., Wang, Q.A., Hepler, C., Vishvanath, L., et al., 2016. Zfp423 maintains white adipocyte identity through suppression of the beige cell thermogenic gene program. Cell Metabolism 23(6):1167–1184.

[17] Morris, A.D., Cordi, A.A., 1997. A new, efficient, two step procedure for the preparation of the antineoplastic agent sparfosic acid. Synthetic Communications 27(7):1259–1266.

[18] Jones, M.E., 1970. Regulation of pyrimidine and arginine biosynthesis in mammals. Advances in Enzyme Regulation 9:19–49.

[19] Grem, J.L., King, S.A., O'Dwyer, P.J., Leyland-Jones, B., 1988. Biochemistry and clinical activity of N-(phosphonacetyl)-L-aspartate: a review. Cancer Research 48(16):4441–4454.

[20] Wang, Z.V., Deng, Y., Gao, N., Pedrozo, Z., Li, D.L., Morales, C.R., et al., 2014. Spliced X-box binding protein 1 couples the unfolded protein response to hexosamine biosynthetic pathway. Cell 156(6):1179–1192.

[21] Peters, G.J., van Groeningen, C.J., Laurensse, E.J., Lankelma, J., Leyva, A., Pinedo, H.M., 1987. Uridine-induced hypothermia in mice and rats in relation to plasma and tissue levels of uridine and its metabolites. Cancer Chemotherapy and Pharmacology 20(2):101–108.

[22] (a) Sriburi, R., Jackowski, S., Mori, K., Brewer, J.W., 2004. XBP1: a link between the unfolded protein response, lipid biosynthesis, and biogenesis of the endoplasmic reticulum. The Journal of Cell Biology 167(1):35–41.
(b) Cox, J.S., Chapman, R.E., Walter, P., 1997. The unfolded protein response coordinates the production of endoplasmic reticulum protein and endoplasmic reticulum membrane. Molecular Biology of the Cell 8(9):1805–1814.

[23] Ng, B.G., Wolfe, L.A., Ichikawa, M., Markello, T., He, M., Tifft, C.J., et al., 2015. Biallelic mutations in CAD, impair de novo pyrimidine biosynthesis and decrease glycosylation precursors. Human Molecular Genetics 24(11):3050–3057.

[25] (a) Reimold, A.M., Iwakoshi, N.N., Manis, J., Vallabhajosyula, P., Szomolanyi-Tsuda, E., Gravallese, E.M., et al., 2001. Plasma cell differentiation requires the transcription factor XBP-1. Nature 412(6844):300–307.
(b) Lee, A.H., Chu, G.C., Iwakoshi, N.N., Glimcher, L.H., 2005. XBP-1 is required for biogenesis of cellular secretory machinery of exocrine glands. The EMBO Journal 24(24):4368–4380.

[26] Romero-Ramirez, L., Cao, H., Nelson, D., Hammond, E., Lee, A.H., Yoshida, H., et al., 2004. XBP1 is essential for survival under hypoxic conditions and is required for tumor growth. Cancer Research 64(17):5943–5947.

[27] Reardon, M.A., Weber, G., 1985. Increased carbamoyl-phosphate synthetase II concentration in rat hepatomas: immunological evidence. Cancer Research 45(9):4412–4415.

[28] Huang, M., Kozlowski, P., Collins, M., Wang, Y., Haystead, T.A., Graves, L.M., 2002. Caspase-dependent cleavage of carbamoyl phosphate synthetase II during apoptosis. Molecular Pharmacology 61(3):569–577.

[29] Gill, B.D., Indyk, H.E., 2007. Determination of nucleotides and nucleosides in milks and pediatric formulas: a review. Journal of AOAC International 90(5):1354–1364.

[30] Smith, K.A., Agarwal, M.L., Chernov, M.V., Chernova, O.B., Deguchi, Y., Ishizaka, Y., et al., 1995. Regulation and mechanisms of gene amplification. Philosophical Transactions of the Royal Society of London B Biological Sciences 347(1319):49–56.

[31] Wouters, B.G., Koritzinsky, M., 2008. Hypoxia signalling through mTOR and the unfolded protein response in cancer. Nature Reviews Cancer 8(11):851–864.

[32] Sha, H., Yang, L., Liu, M., Xia, S., Liu, Y., Liu, F., et al., 2014. Adipocyte spliced form of X-box-binding protein 1 promotes adiponectin multimerization and systemic glucose homeostasis. Diabetes 63(3):867–879.

[33] Koc, M., Mayerova, V., Kracmerova, J., Mairal, A., Malisova, L., Stich, V., et al., 2015. Stress of endoplasmic reticulum modulates differentiation and lipogenesis of human adipocytes. Biochemical and Biophysical Research Communications 460(3):684–690.

[34] Domingo, P., Torres-Torronteras, J., Pomar, V., Giralt, M., Domingo, J.C., Gutierrez Mdel, M., et al., 2010. Uridine metabolism in HIV-1-infected patients: effect of infection, of antiretroviral therapy and of HIV-1/ART-associated lipodystrophy syndrome. PLoS One 5(11):e13896.

